Journal of Orthopaedic Translation 50 (2025) 306–332

Contents lists available at ScienceDirect

Journal of Orthopaedic Translation

journal homepage: www.journals.elsevier.com/journal-of-orthopaedic-translation

Review Article

Design of internal fixation implants for fracture: A review

Heng Zhang [a], Shipeng Xu [b], Xiaohong Ding [a,*], Min Xiong [a], Pengyun Duan [a]

[a] School of Mechanical Engineering, University of Shanghai for Science and Technology, No. 516 Jungong Road, Shanghai, 200093, China
[b] Shanghai Institute of Special Equipment Inspection and Technical Research, No.915 Jinshajiang Road, Shanghai, 200062, China

ARTICLE INFO

Keywords:
Additive manufacturing
Evaluation method
Fracture healing
IFI design
Internal fixation implant
Surface treatment

ABSTRACT

Internal fixation is the most common and effective fracture treatment, and the design of Internal Fixation Implants (IFI) is important for fracture healing. In recent decades, IFI have been designed from the aspects of materials, geometry, fixation methods and functional characteristics. However, there has been no comprehensive summary on the evaluation method and design methods of IFI. This paper aims to review and analyze the key issues involved in the design of IFI, to provide references for IFI design. Firstly, the main factors affecting the healing effect are summarized and the design requirements of IFI are put forward through the analysis of fracture healing process. Secondly, the evaluation methods of IFI are compared and summarized, and the importance of evaluation methods based on fracture healing theory is emphasized. Subsequently, the properties and application scopes of common biomaterials for IFI are introduced. And the IFI, which is used widely, such as bone plate, intramedullary nail and embracing device, are summed up from the aspects of design factors and design methods. Highlight the distinctive contributions of additive manufacturing for the fabrication of implants and surface treatment for improving the multifunctionality of implants. Finally, the design concept of ideal IFI and the potential research content in the future are proposed based on the design requirements and the summary of the existing design studies.

The translational potential of this article: This study summarizes and analyzes the key issues involved in the design of IFI, which provide references for IFI design. A discussion on future research directions and suggestion were made, which is expected to advance the research in this field.

1. Introduction

Bone fracture is a common traumatic disease, and its treatment generally needs to choose the fixation mode according to the fracture location and type. There are two types of fracture fixation mode: external fixation and internal fixation. The external fixation generally uses splints, plaster bandages or external fixator [1]. While the internal fixation mainly uses bone plate, screw, intramedullary nail or embracing device [2]. In recent decades, internal fixation technology has been developing and innovating in the aspects of fixation theory, fixation principle, IFI design and implantation method [3]. Internal fixation has become the most commonly used fracture treatment methods by establishing accurate reduction, providing stable fixation and preserving bone blood supply as much as possible to achieve a satisfactory clinical treatment effect [4,5].

After fixation, the broken bone, IFI and auxiliary parts form a complex system. Its complexity is mainly manifested that the fracture healing requires reasonable biomechanical stimulation, while the magnitude of biomechanical stimulation is closely related to callus stiffness, IFI stiffness and fixation form. The change of callus stiffness is non-linear with time during fracture healing process which roughly includes the stages of soft callus, hard callus and callus remodeling. This strong coupling nonlinear relationship between multiple components with different materials makes it difficult to design IFI, in which the reasonable mechanical stimulation should be produced in different healing stages. With the continuous progress of material science, manufacturing technology and medical technology, the IFI have made great progress from simple screws and metal bone plates to locking compression bone plate, shape memory implant and intramedullary nail. However, how to design IFI to achieve the better healing effect for different fracture situation remains to be further studies and exploration.

In this paper, the research progress and related key issues of IFI design are reviewed and analyzed in order to provide references for IFI design. The organizational structure and section arrangement of the paper are shown in Fig. 1. Section 2 summarizes the design requirements

* Corresponding author.
E-mail address: dingxh@usst.edu.cn (X. Ding).

https://doi.org/10.1016/j.jot.2024.09.012
Received 5 November 2023; Received in revised form 29 August 2024; Accepted 29 September 2024

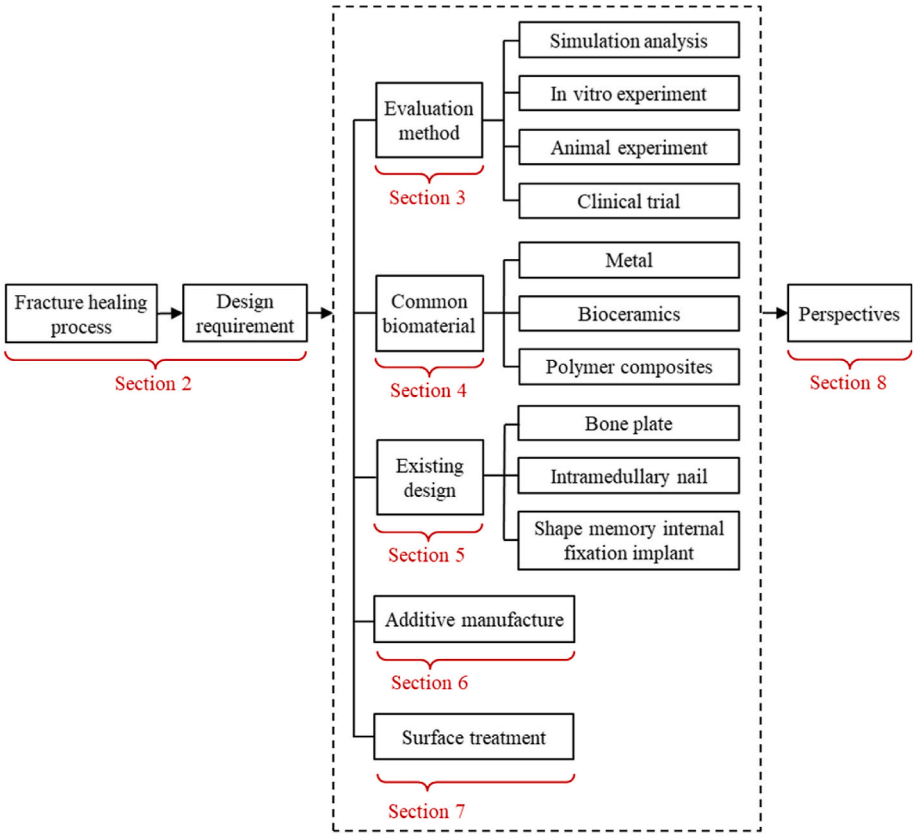

Fig. 1. Organizational structure and section arrangement of the paper.

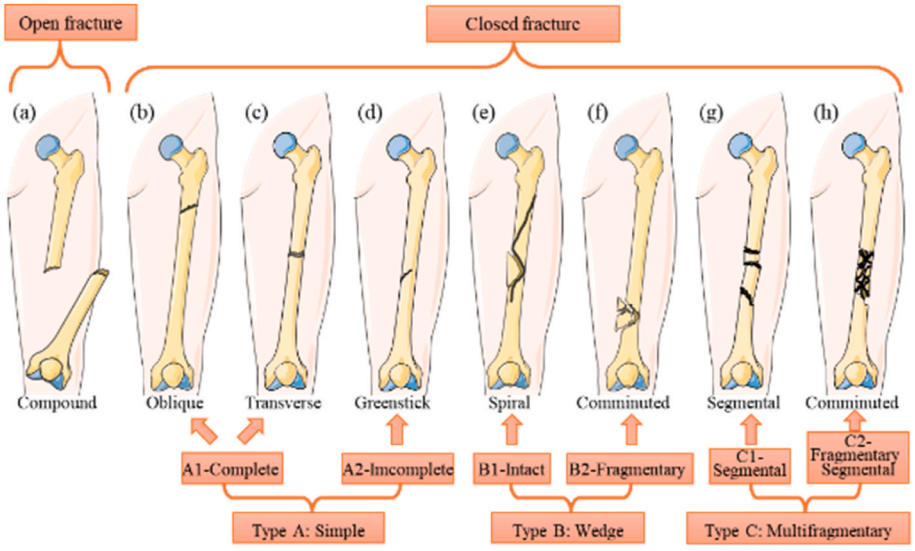

Fig. 2. Bone fracture types. This figure was created using Servier Medical Art templates, which are licensed under a Creative Commons Attribution 3.0 Unported License (https://creativecommons.org/licenses/by-sa/3.0/legalcode); https://smart.servier.com.

of IFI according to the biological and biomechanical characteristics of fracture healing. Sections 3-5 analyze and discuss the evaluation methods, commonly used biomaterials, and existing design studies of IFI, respectively. Section 6 discuss the new trends in additive manufacturing for IFI design and manufacture, Section 7 summarizs the surface treatment for IFI. Finally, the prospect and the potential research content in future are put forward in section 8.

2. Design requirements for IFI

A fracture is a partial or complete break in the bone. When a fracture happens, it's classified as either open or closed. Open fracture (compound fracture): The bone pokes through the skin and can be seen. Or a deep wound exposes the bone through the skin, as shown in Fig. 3(a). Closed fracture: The bone is broken, but the skin is intact, in most cases, the bone fracture is closed fracture. In addition, take diaphyseal fracture for instance, the bone fractures can be further sub-classified as: Simple-

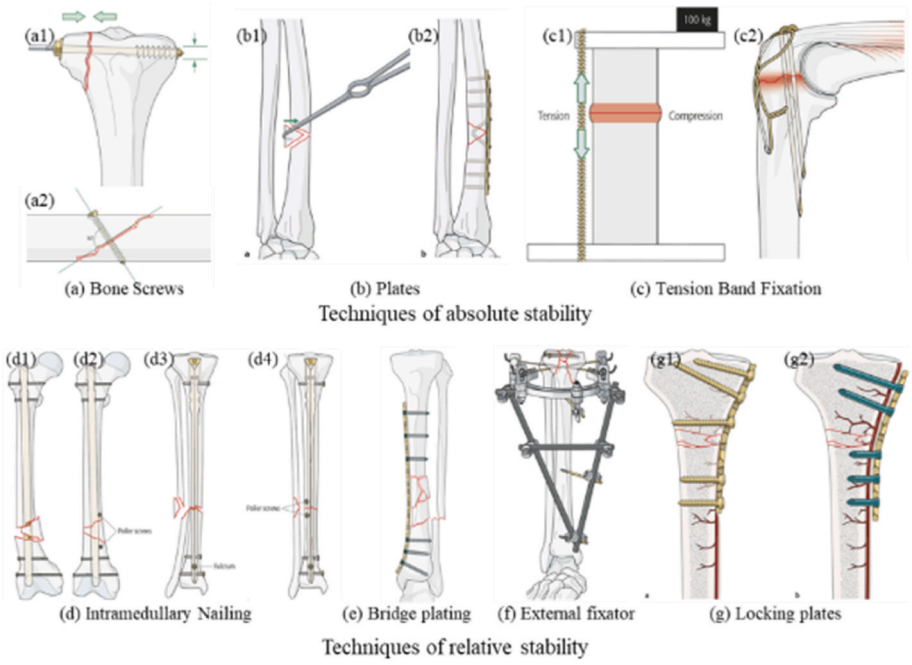

Fig. 3. Fixation techniques [3]. Copyright by AO Foundation, Switzerland.

type A, Wedge-type B and Multifragmentary-type C [3].

1. Simple fractures type A

A fracture can be complete, breaking into two pieces, or incomplete. It can be divided into two groups:

● Complete fracture

The bone is broken in two pieces, such as, oblique fracture shown in Fig. 3(b) (greater than or equal to 30°to a line perpendicular to the long axis of the bone), transverse fracture shown in Fig. 3(c) (greater than or equal to 30° to a line perpendicular to the long axis of the bone).

● Incomplete fracture

The typical incomplete fracture is greenstick fracture which is shown in Fig. 3(d). A greenstick fracture is a partial thickness fracture where only the cortex and periosteum are interrupted on one side of the bone but remain uninterrupted on the other.

2. Wedge fractures type B

The bone is fractureed into one or more intermediate fragments. After reduction there is some cortical contact between the main proximal and distal fragments. Wedge fractures are divided into two groups:

● Intact wedge fracture

There is a single wedge fragment, for example, the spiral fracture as shown in Fig. 3(e).

● Fragmentary wedge fracture

There is more than one wedge fragment, for example the comminuted fracture shown in Fig. 3(f).

3. Multifragmentary fractures type-C

The bone is also broken in one or more intermediate fragments. The difference with type B is that after reduction there is no contact between the main proximal and distal fragments. It also has two groups:

● Intact segmental fracture

They happen when one of your bones is broken in at least two places,

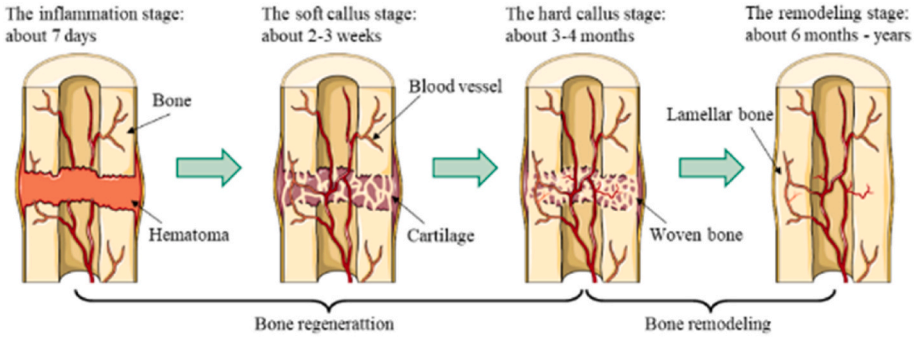

Fig. 4. Different stages of indirect healing [6,9]. This figure was created using Servier Medical Art templates, which are licensed under a Creative Commons Attribution 3.0 Unported License (https://creativecommons.org/licenses/by-sa/3.0/legalcode); https://smart.servier.com.

Table 1
Material properties of different types of tissue [10].

Property	Granulation tissue	Fibrous tissue	Cartilage	Immature bone	Mature bone	Cortical bone	Marrow
Young's modulus (MPa)	1	2 [18]	10 [19]	1000	6000 [20]	$E_r = 8500$ $E_0 = 7000$ $E_z = 1575$ [21]	2
Permeability (m^4/Ns)	10^{-14}	10^{-14} [18]	5×10^{-15} [22]	10^{-13}	3.7×10^{-13} [23]	10^{-17} [24]	10^{-14}
Poisson's ratio	0.167	0.167	0.167 [25]	0.325	0.325	0.325 [26]	0.167
Solid bulk modulus (MPa)	2300 [27]	2300	3400 [28]	17660 [29]	17660 [29]	17660 [29]	2300
Fluid bulk modulus (MPa)	2300	2300	2300	2300	2300	2300	2300
Porosity	0.8	0.8	0.8 [30]	0.8	0.8	0.04 [31]	0.8

leaving a segment of your bone totally separated by the breaks. as shown in Fig. 3(g)

- Fragmentary segmental fracture

The bone is broken in several irregular intermediate fragments, as shown in Fig. 2(h).

According to whether the relative micro-movement can generate in the interfragmentary gap after fixation, internal fixation is divided into two types, one is absolute stable fixation and the other is relative stable fixation [6]. In the case of absolute stable fixation, which is a fixation method based on mechanics, the ends of fracture bone are closely connected under the fixation of IFI and there is no relative micro-movement under the load. Typical absolute stable fixation methods include the bone screws (Fig. 3 (a)), plates (Fig. 3 (b)) and tension band fixation (Fig. 3 (c)) to fix the fractured bone. The fracture will heal directly by the action of osteoclasts and osteoblasts, also known as primary healing which has no callus formation. The relatively stable fixation is based on biological fixation and allowed to produce relative micro-movement under the load. The relatively stable fixation methods include intramedullary nailing (Fig. 3 (d)), brindge plating (Fig. 3 (e)), external fixator (Fig. 3 (f)) and locking plate (Fig. 3 (f)), and so on. In this case, the callus generates at the fracture site first and then restore to healthy bone state through bone remodeling. This form of fracture healing is called indirect or secondary healing [7]. The absolutely stable fixation is easy to cause the rupture of IFI due to stress concentration and cause secondary injury. While in the relatively stable fixation state, IFI are not prone to rupture because of stress dispersion, and mechanical stimulation can generate at the fracture site to effectively promote fracture healing [8]. Therefore, the relatively stable internal fixation has become the most commonly used form in recent years.

Fracture healing is a complex biological process, as shown in Fig. 4, indirect healing which includes bone regeneration and bone remodeling can be divided into four stages: the inflammation stage, the soft callus stage, the hard callus stage and the remodeling stage [6,9]. The inflammatory stage lasted for about 7 days, and the rupture of blood vessels causes a hematoma which is gradually replaced by granulation tissue. In the soft callus stage, which lasts for 2–3 weeks, the capillaries grow into callus and the cartilage is generated by the proliferating, migrating and differentiating of mesenchymal stem cells. Subsequently, the cartilage is ossified into woven bone and fracture bone is bridged by hard callus in the hard callus stage which lasts 3–4 months. The callus remodeling stage takes months to years, in which the woven bone is remodeled into lamellar bone and the bone gradually recovers to its original state. The material properties of different tissues [10] are shown in Table 1. From granulation tissue to cartilage, the elastic modulus increases from the initial 1 MPa to about 10 MPa. With the progress of cartilage ossification, the elastic modulus reaches 6000 MPa when grown into mature bone. After that, the callus recovered to cortical bone through bone remodeling, and the elastic modulus reached 8000 MPa. The solid bulk modulus increases from granulation tissue, fibrous tissue, cartilage, immature bone and mature bones. Different with indirect bone healing, direct healing is achieved through lamellar bone formation, blood vessels, and the formation of Haversian canals. This is

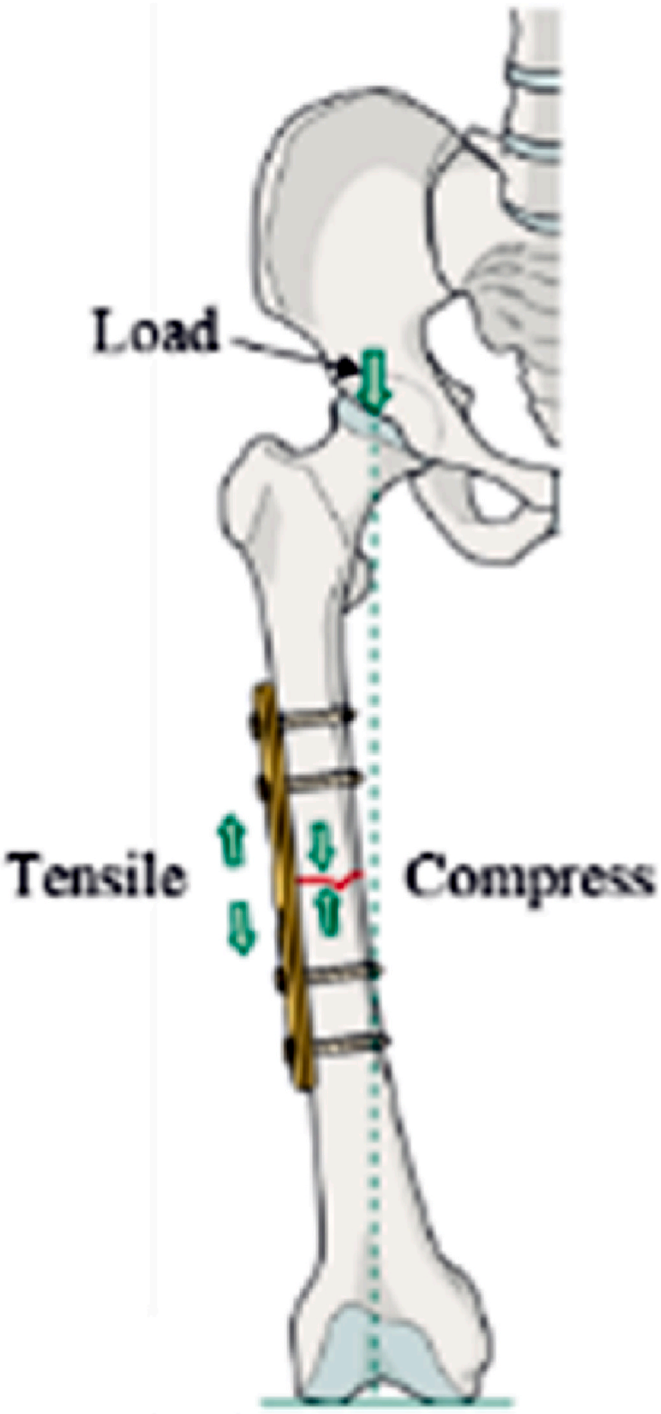

Fig. 5. Femoral fracture fixed with bone plate and screws [3]. Copyright by AO Foundation, Switzerland.

Table 2
Evaluation contents and characteristics of common IFI evaluation methods.

Method	Content	Characteristic
Simulation analysis	Mechanical properties of IFI, Mechanical stability of the fixation system, Fracture healing effect	Fast evaluation and low cost.
In vitro experiment	Mechanical properties of IFI, Mechanical stability of the fixation system	Only mechanical properties.
Animal experiment	Biocompatibility, Fracture healing effect	Intuitive, but biological characteristics differences between the animals and humans.
Clinical trials	Biocompatibility, Fracture healing effect	Most effective, but differences among individual patients, high time cost.

surgically accomplished through a contact healing or gap healing processes without the formation of callus. Generally, indirect (secondary) bone healing: occurs due to mechanical stimulation (relative stability) of interfragmentary movement (2–10 % strain); while direct (primary) bone healing: occurs in the present of absolute stability (i.e., little or no movement of the fracture fragments—0 to 2 % strain) [11]. The generation and remodeling of callus requires reasonable biomechanical stimulation, and the magnitude of biomechanical stimulation is affected by various factors, such as load [12], fracture type and the stiffness of IFI [13–16]. Different post-surgery rehabilitation exercises lead to different load and stimus, which results in different bone fracture healing performance. Appropriate levels of torsion are essential for the successful healing of bone fractures.Taking the transverse fracture of femoral shaft fixed by bone plate and screws as an example in Fig. 5, the bone plate and the fractured bone are in the states of tension and compression respectively under the action of load. The mechanical stimulation at the fracture site is comprehensively affected by the magnitude of the load, the fracture situation, the stiffness of bone plate, the layout of the screws and so on. In addition, the contact between the bone plate and the bone may damage the periosteal capillary network and disrupt the blood supply, affecting the healing of fracture [17]. Therefore, a reasonable design of IFI is important to provide the mechanical stimulation required for fracture healing.

Through the above analysis, the design requirements of IFI are summarized as follows: (1) made by materials with good biocompatibility, (2) has enough stiffness for accurate reduction of fracture bone and sufficient fixation stability, (3) produce reasonable and continuous biomechanical stimulation at the fracture site in the process of fracture healing, (4) has as small as possible contact area between IFI and bone to protect the blood supply.

3. Evaluation methods for IFI

The fixation effect needs to be evaluated to guide the improvement and optimization of IFI design. The evaluation methods mainly include simulation analysis, in vitro experiments, animal experiments and clinical trials. The contents and characteristics of different evaluation methods are listed in Table 2. The simulation analysis, which has the characteristics of fast evaluation and low cost, can be used to evaluate not only the mechanical properties of IFI and the mechanical stability of fixation system but also the healing effect by simulating the process of fracture healing [32]. By in vitro experiments, however, just only can evaluate the mechanical properties of IFI and the mechanical stability of fixation system. In addition, the material properties of artificial bone which is often used in vitro experiments are different from those of real bone [33]. The biocompatibility of IFI and the fracture healing effect can be evaluated by animal experiments, but issues such as the availability of animals, experimental costs, social acceptance, and whether they have similar biological characteristics to humans must be considered [34,35]. Clinical trials are the most intuitive and effective evaluation method to observe the impact of IFI on fracture healing effects, but there are some differences among individual patients and the follow-up time is long [36–38]. The evaluation methods mainly used in the initial design stage are simulation analysis and in vitro experiments, while animal experiments and clinical trials are suitable for the final evaluation and verification.

With the development of biomechanics, computational science and other disciplines, simulation analysis can provide fast and rich evaluation and has become the most important evaluation method in the initial design stage. According to the different evaluation contents, the simulation analysis evaluation methods can be divided into two categories.

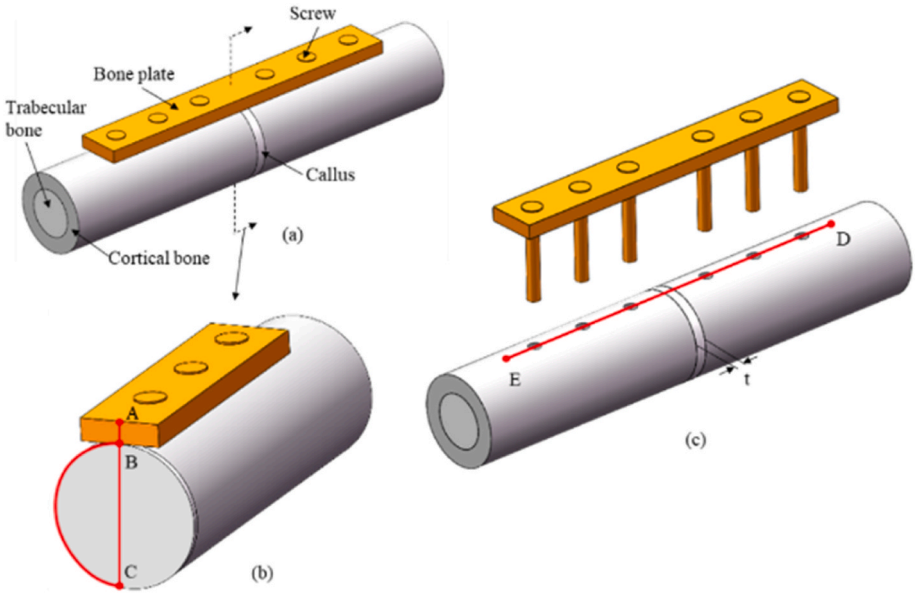

Fig. 6. The bone–bone plate fixation system: (a) Overall assembly [42–44], (b) Sectional view [45,46,48,49], (c) Bone and plate separation [47,50–53].

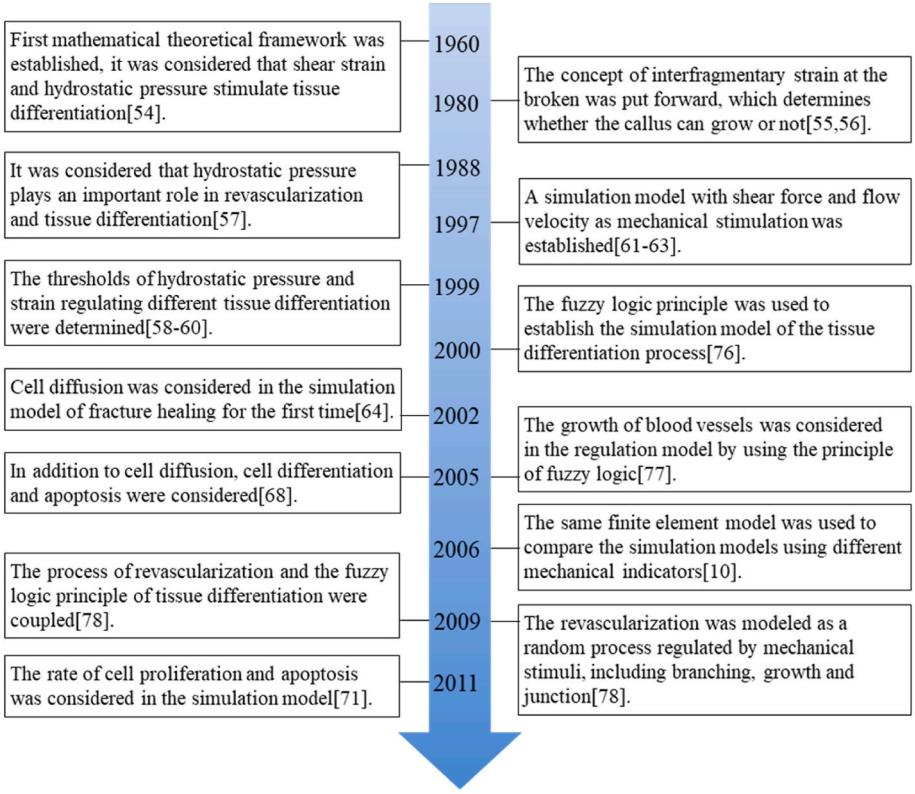

Fig. 7. Development history of bone regeneration simulation model.

One is to analyze the mechanical properties of IFI and the mechanical stability of fixation system. The other is to simulate the generation and remodeling process of callus by establishing mathematical models to evaluate the effect of IFI on fracture healing.

3.1. Fixation stability evaluation

In the evaluation of IFI, the easiest way is to analyze the stress of IFI under normal load and confirm the safety of IFI by judging whether the maximum stress is less than the allowable stress of the used material [39–41]. However, it is difficult to ensure the biomechanical stimulation required for fracture healing is generated at the fracture site if the IFI were designed with structural strength as design objective only. Therefore, it is necessary to select more reasonable evaluation indexes to evaluate the fixation stability. In addition to the stress distribution of bone-IFI system [42–44], the mechanical characteristics of some special positions can also be used as evaluation indexes for fixation stability. Take the bone–bone plate fixation system shown in Fig. 6 as an example, the evaluation indexes commonly used are radial centerline stress distribution of fracture section [45,46], stress distribution at the interface between bone and IFI [47], stress and strain distribution of callus [48,49], and changes of the interfragmentary gap [50–53]. Fig. 6(a) is the overall schematic diagram of the fixation system, and its sectional view is shown in Fig. 6(b). The stress on segment AB and BC in Fig. 6(b) can be used not only to evaluate the fixation stability but also to analyze the stress split of plate and fracture bone by comparing the stress changes in different healing periods [45,46]. The stress or strain on the radial line BC and the circumferential arc BC can quantitatively and intuitively describe the mechanical stimulation on callus [48,49]. Fig. 6(c) shows the separation of bone plate and fractured bone, in which the segment DE is the center line of the contact surface between fracture bone and bone plate, and the stress distribution on DE can roughly judge whether the bone is damaged. The size of the interfragmentary gap is shown as t in Fig. 6(c), the change of t under load can quantify the mechanical stimulation on callus and evaluate the fixation stability [50–53].

3.2. Bone regeneration simulation model

In order to meet the design requirements of the IFI, a comprehensive evaluation which includes the safety of IFI, the fixation stability and the mechanical stimulation on callus should be developed when designing IFI. The callus is generated in bone regeneration stage. Relevant scholars have established simulation models to simulate the bone regeneration process, and the effect of IFI on bone regeneration was evaluated by simulation to provide guidance for IFI design. According to whether biological factors are considered, bone regeneration simulation models can be divided into two categories: biomechanical regulation model and biomechanical-biological regulation model. The main development process of bone regeneration simulation model is shown in Fig. 7.

3.2.1. Biomechanical regulation model

In 1960, Pauwel et al. [54] thought that shear strain and hydrostatic pressure stimulate the differentiation of mesenchymal stem cells and established the first mathematical theoretical framework, as shown in Fig. 8(a), to describe the differentiation of callus under the regulation of mechanical stimulation. This theory is based on clinical observation and could not measure the shear strain and hydrostatic pressure in detail. In 1988, Carter et al. [55,56] formulated a theory framework for predicting tissue differentiation. As shown in Fig. 8(b), the hydrostatic stress and the principal strain are considered as the main factors affecting revascularization and tissue differentiation.

The above models only studied the stimulating effect of different mechanical factors on callus growth but did not determine the threshold of specific mechanical stimulation for promoting the growth of different tissue. In 1980, Perren et al. [57] proposed the concept of interfragmentary strain, as shown in Fig. 8(c), and believed that the interfragmentary strain between 2 % and 10 % can stimulate the formation of cartilage. Although the interfragmentary strain theory provides a

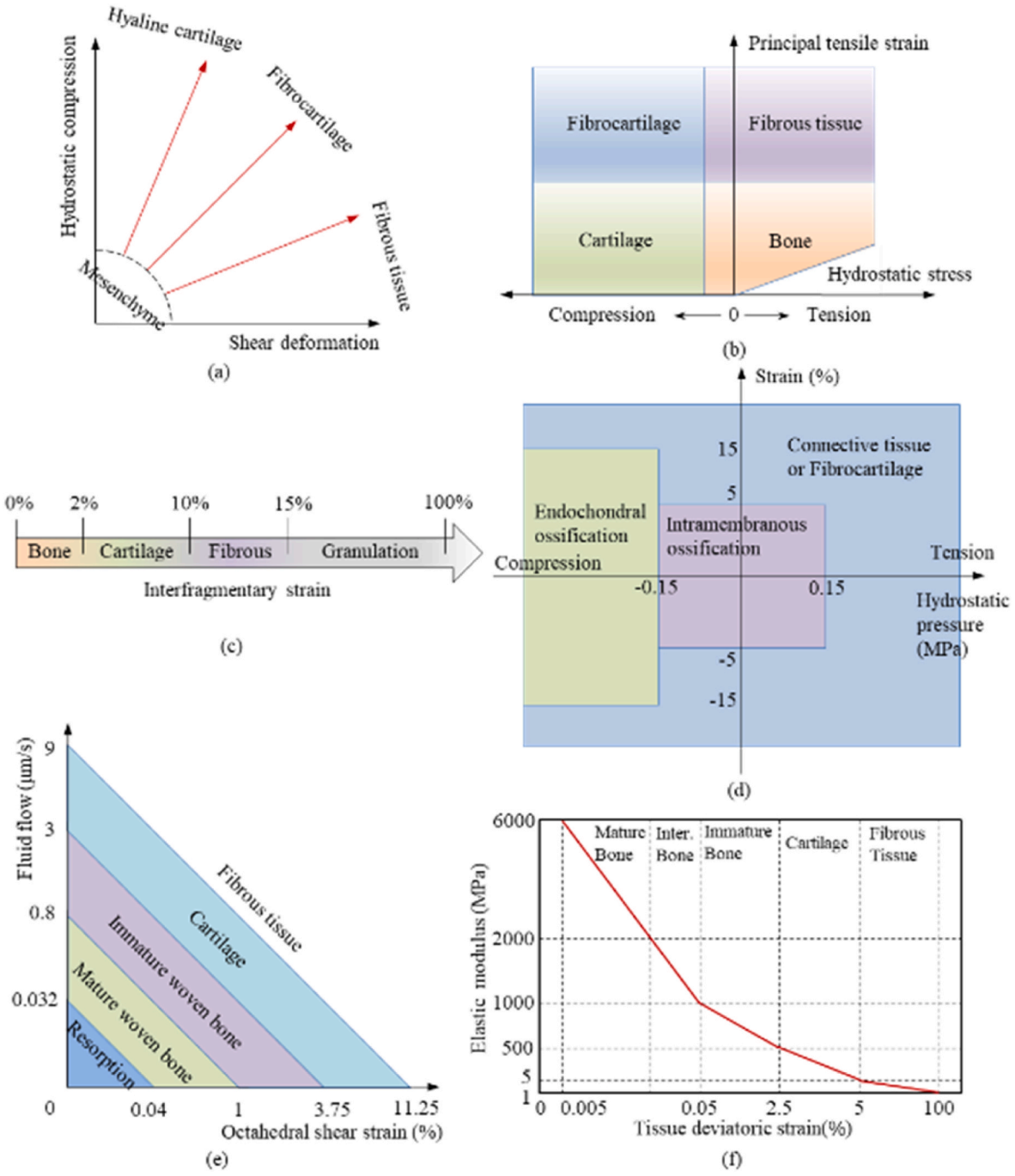

Fig. 8. Bone regeneration simulation model: (a) Shear deformation and hydrostatic compression [54], (b) Hydrostatic stress and principal tensile strain [55,56], (c) Interfragmentary strain [57], (d) Hydrostatic pressure and strain [20,58,59], (e) Octahedral strain and fluid flow [60–63], (f) Deviatoric strain [10].

method for IFI evaluation, it ignores the radial and hoop shear forces experienced by the callus and could not predict the continuous fracture healing process. Claes et al. [20,58,59] used a combination method of animal experiments, cell culture and finite element analysis, to quantify the range of mechanical stimulations that stimulates different tissue differentiation. As shown in Fig. 8(d), the intramembrane ossification could be stimulated when the hydrostatic pressure is between -0.15 ~ 0.15MPa and the octahedral shear strain is between −5% and 5 %. The cartilage ossification could be stimulated when the hydrostatic pressure is less than −0.15 MPa and the octahedral shear strain is between −15 %–15 %. And the cartilage formation could be promoted when both the hydrostatic pressure and the octahedral shear strain are outside the above range.

3.2.2. *Biomechanical-biological regulation model*

The effects of different mechanical factors on bone regeneration could be studied by the biomechanical regulation model. To simulate a more real bone regeneration process, some scholars have established bone regeneration simulation models considering both biomechanical and biological factors.

The biological factors in the bone regeneration simulation model mainly include cell activity and vascular remodeling, in which cell activity mainly manifests as cell migration, differentiation and proliferation. Prendergast et al. [60–63] used diffusion analysis to describe the migration of mesenchymal stem cells, and simulated the continuous bone regeneration process on the time course. As shown in Fig. 8(e), they suggested that the formation of fibrous tissue is stimulated when

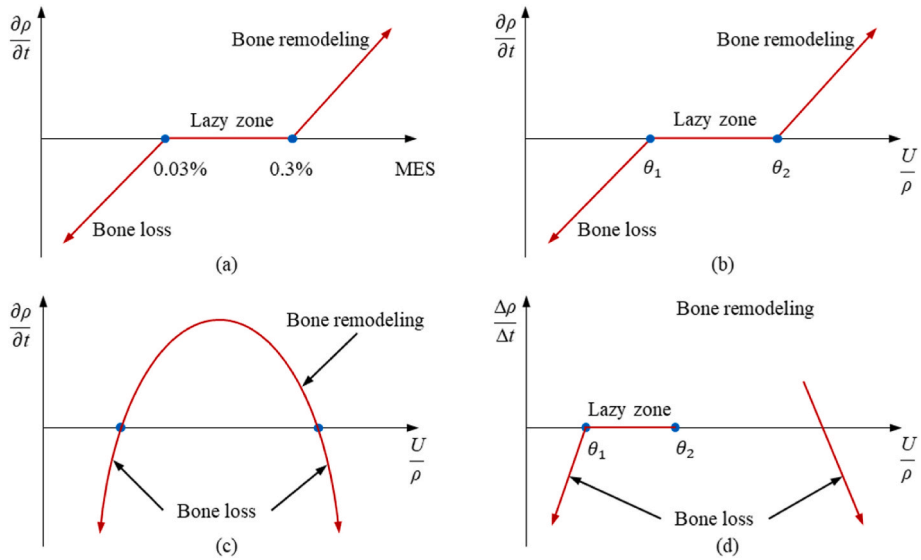

Fig. 9. Bone remodeling simulation model:(a) MES [80–82], (b) SED and without considering overload [83],(c) SED and without considering lazy zone [86],(d) SED with considering both overload and lazy zone [87].

the shear strain is greater than 11.25 % and the flow rate is greater than 9 μm/s, the formation of cartilage is stimulated when the shear strain is between 3.75% and 11.25 % and the flow rate is greater than 3 μm/ s-9 μm/s. And cartilage ossification is stimulated when the shear strain is between 0.04% and 3.75 % and the flow rate is between 0.03 μm/ s-3 μm/s. The callus is absorbed when the shear strain is less than 0.04 % and the flow rate is less than 0.03 μm/s. Subsequently, Perez et al. [64] used a random-walk model to simulate the proliferation of mesenchymal stem cells, which could generate different tissue distribution states compared to the diffusion analysis.

The finite element models used in the above studies are different, so it is impossible to directly compare the simulation results of different simulation models. In 2006, Isaksson et al. [10] used the same finite element model to compare the simulation models considering cell migration with different mechanical indicators. They found that different simulation models can correctly simulate the bone regeneration process and there are some insignificant differences in the results. Further study found that the simulation model with deviatoric strain as mechanical stimulation could accurately simulate the normal bone regeneration process, and the results were verified by animal experiments [65]. As shown in Fig. 8(f), the formation of fibrous tissue and cartilage are stimulated when the deviatoric strain are greater than 5 % and between 2.5% and 5%, respectively. Cartilage ossification and the formation of mature bone are stimulated when the deviatoric strain are between 0.05%-2.5 % and 0.005%–0.05 %, respectively. And the callus is absorbed when the deviatoric strain is less than 0.005 %. Subsequently, Isaksson et al. [66] simulated the distribution of different types of callus during bone regeneration by establishing a nonlinear partial differential equation system to couple the cell differentiation with mechanical stimulation. Based on the above studies, Kelly et al. [67] established a simulation model that simultaneously considered cell migration, differentiation and apoptosis, making the simulation process more realistic.

During bone regeneration, the volume of callus increases gradually. Gomez et al. [68,69] simulated the change of callus volume during bone regeneration by thermoelastic analysis, and analyzed the changes of callus geometry, tissue differentiation mode and callus stiffness with different interfragmentary gap under different loads. Based on the study of Gomez et al. [68,69], Kang et al. [70] studied the regulating effect of the magnitude and frequency of mechanical stimulation on the rate of cell proliferation and apoptosis. Isaksson et al. [71] characterized bone regeneration by the increase of callus volume and simulated the spatial and temporal distribution of callus during bone regeneration, where the rate of volume increase was dependent on the rate of matrix production.

To study the mathematical relationship between mechanical stimulation and bone regeneration, Garcia-Aznar et al. [72] established a continuous mathematical model to simulate bone regeneration by taking the second invariant of partial strain tensor as mechanical stimulation. And the influence of micro-movement on the generation and final morphology of callus was analyzed. Subsequently, Reina-Romo et al. [73,74] applied a continuous mathematical model to the study of dispersed osteogenesis and analyzed the effect of dispersion rate on osteogenesis. Due to the biological complexity of bone regeneration, Ament et al. [75] proposed a fuzzy controller to simulate the bone regeneration process with considering the uncertainty of the relationship between bone regeneration and mechanical stimulation. The principle of fuzzy logic was obtained from relevant medical theories.

In addition to cell activity, revascularization is another important factor affecting bone regeneration. Shefelbine et al. [76] developed a simulation model considering revascularization by using fuzzy logic principles. Chen et al. [77] divided revascularization into two independent processes, which are vascular growth and nutrient supply, and combined the revascularization with bone regeneration using diffusion analysis. Simon et al. [78] introduced revascularization as a space-time variable into the dynamic model to study the interaction between revascularization and tissue differentiation during bone regeneration. Based on the research of Prendergast et al. [62], Checa et al. [79] modeled the revascularization, which includes vascular growth, branching and junction, as a random process regulated by mechanical stimulation.

In conclusion, the bone regeneration simulation model has developed from a theoretical framework based on biomechanics to the biomechanical-biological model considering biomechanical stimulation, cell activity and revascularization. The evaluation method based on bone regeneration simulation model can guide the IFI design to meet the biomechanical requirements of callus generation.

3.3. *Bone remodeling simulation model*

The fracture bone can recover to healthy bone through bone remodeling after callus generation. Relevant scholars have established the bone remodeling simulation model to describe the impact of biomechanical stimulation on bone remodeling. Frost et al. [80–82] believed that the bone remodeling process is regulated by the minimum

Table 3
The types and main applications of common biomaterials for IFI.

Type			Elastic modulus (GPa)	Main applications	Reference
Metal	Non-biodegradable metal	Stainless steel, titanium alloy, cobalt alloy, etc.	80–240	Bone plates, intramedullary nails, screws, prostheses, dental implants, cardiovascular stents, spinal IFI, etc.	[90,91]
	Biodegradable metal	Magnesium-based alloys, iron-based alloys, zinc-based alloys, etc.	40–220		
	Shape memory alloy	Nitinol alloy	30–80	Embracing devices, intramedullary nails, pressure nails, cardiovascular stents, etc.	[92]
	Porous functional material	Titanium alloy, tantalum alloy, etc.	10–110	Bone scaffold, prostheses, etc.	[93]
Ceramic	Bio-inert ceramic	Zirconia, alumina	35–380	Bone scaffold, prostheses, dental implants, etc.	[94,95]
	Bio-active ceramic	Calcium phosphate			
Polymer and polymer-based composites	Non-degradable	Carbon fiber/Epoxy, Glass fiber/Epoxy, Glass fiber/polypropylene	0.4–130	Bone plates, intramedullary nails, screws, prostheses, dental implants, cardiovascular stents, spinal IFI, etc.	[96,97]
	Fully degradable	Polyglycolic acid(PGA), polylactic acid (PLA), fiber-reinforced biodegradable composites			[98,99]
	Partially degradable	Non-degradable and fully degradable blend			[100]

effective strain (MES). As shown in Fig. 9(a), bone remodeling occurs when the MES of callus is greater than 0.3 %, maintains the status when MES is between 0.03% and 0.3 %, and degenerates when MES is less than 0.03 %. On the other hand, the strain energy density (SED) was considered to be an important factor affecting bone remodeling [83–85]. Weinans et al. [83] established a bone remodeling simulation mathematical model using SED as mechanical stimulation as follows:

$$\frac{\partial \rho}{\partial t} = \begin{cases} \mathrm{B}\left(\frac{U}{\rho} - \theta_2\right), \frac{U}{\rho} > \theta_2 \\ 0, \theta_1 \le \frac{U}{\rho} \le \theta_2 \\ \mathrm{B}\left(\frac{U}{\rho} - \theta_1\right), \frac{U}{\rho} < \theta_1 \end{cases} \quad (1)$$

$$\theta_1 = (1 - \mathrm{s})\mathrm{k} \quad (2)$$

$$\theta_2 = (1 + \mathrm{s})\mathrm{k} \quad (3)$$

Where ρ is the density of bone, t is time, the constant B represents bone remodeling rate, U is strain energy density, θ_1 and θ_2 are the threshold of mechanical stimulation, the constant s is the width of the lazy zone, and k is the relevant reference value. The curve description is shown in Fig. 9 (b), the bone density decreases when SED is less than θ_1 and the callus is absorbed. When SED is greater than θ_2, the bone density increases and bone remodeling occurs. The bone density dose not change when SED is greater than θ_1 and less than θ_2.

Li et al. [86] explained the effect of overload on bone remodeling by adding a quadratic term to the mathematical model. The mathematical relationship between the rate of bone density change and mechanical stimulation is as follows:

$$\frac{\partial \rho}{\partial t} = \mathrm{B}\left(\frac{U}{\rho} - \theta_2\right) - \mathrm{D}\left(\frac{U}{\rho} - \theta_2\right)^2 \quad (4)$$

The constant D represents bone remodeling rate. The curve description is shown in Fig. 9(c). When SED is too large, the change rate of bone density is negative indicated that bone resorption occurs under overload.

Subsequently, Rungsiyakull et al. [87] established a mathematical model of adaptive bone remodeling considering both lazy and overload interval as follows:

$$\Delta\rho = \begin{cases} \mathrm{B}\left(\frac{U}{\rho} - \theta_2\right)\Delta t - \mathrm{D}\left(\frac{U}{\rho} - \theta_2\right)^2 \Delta t, \frac{U}{\rho} > \theta_2 \\ 0, \ \theta_1 \le \frac{U}{\rho} \le \theta_2 \\ \mathrm{B}\left(\frac{U}{\rho} - \theta_1\right)\Delta t, \frac{U}{\rho} < \theta_1 \end{cases} \quad (5)$$

As shown in Fig. 9(d), when SED is too small or too large, the callus is absorbed. The callus remains in the current state when SED is in the lazy interval. And bone remodeling can carry out only when SED is in the appropriate interval.

The impact of mechanical stimulation on bone remodeling can be intuitively reflected by the simulation of bone remodeling. The evaluation method based on bone remodeling simulation model can provide important biomechanical reference value for the design of IFI.

Although the current researches on the simulation models of bone regeneration and bone remodeling have been relatively mature and comprehensive, it is still lack of a combined model of bone regeneration and bone remodeling for simulating the continuous process of bone fracture healing.

4. Commonly used biomaterials for IFI

The IFI should be made by material with good biocompatibility, and the common biomaterials are mainly divided into three categories: metal, ceramic and polymer [88,89]. With the development of material science, some biomaterials with specific functions have been appeared, such as biodegradable materials, shape memory alloys and porous functional materials. New materials have attracted more and more attention because of their unique functional characters. The types and main applications of common biomaterials for IFI are shown in Table 3.

4.1. Metal

4.1.1. Non-biodegradable metal

The non-biodegradable metals, such as stainless steel, titanium alloys and chromium-cobalt alloys, are usually used for traditional IFI [101]. Non-biodegradable metals have good biocompatibility, high wear resistance and excellent mechanical properties, so they are still the most commonly used biomaterial for IFI. However, the elastic modulus of non-biodegradable metal is 10–20 times that of cortical bone, which may cause stress shielding resulting in bone nonunion, osteoporosis, and even secondary fracture [102,103]. Moreover, permanent drilling may cause chronic inflammation due to the long-term existence of IFI in the

body [104–106], and secondary surgery is needed when removing IFI [107]. In addition, when X-ray and computed tomography (CT) are used for diagnosis, non-degradable metal IFI causes beam hardening and image artifacts affecting the accuracy of diagnosis [108].

4.1.2. Biodegradable metal

To overcome the limitations of non-degradable metals, relevant researchers used biodegradable metal in IFI design. Biodegradable metals can gradually dissolve in body through host reactions which makes the structural stiffness of IFI gradually decreases, hence the fracture bone gradually bears more load because of the load split [109]. Consequently, the stress shielding effect is reduced and fracture healing is promoted [91].

There are three commonly used biodegradable metal materials: magnesium-based alloy, iron-based alloy and zinc-based alloy [110]. Among them, magnesium-based alloy is used most in IFI design because of its good biocompatibility and mechanical properties, although its application is limited due to its fast degradation rate [111]. Magnesium is a necessary and the fourth most abundant element in human body. It is easy to be absorbed by the human body and discharged from the urine. A series of clinical trials have shown that magnesium can promote fracture healing to a certain extent. The elastic modulus of magnesium-based alloy is close to that of natural bone. When magnesium-based alloy IFI are used for the fracture fixation of non-load bearing bone, not only the sufficient fixation stiffness can be provided but also the stress shielding effect can be reduced. And the mechanical properties of magnesium-based alloys can be changed to a certain extent through alloying, heat treatment, surface coating and other technologies [112, 113].

The degradation rate in vivo of iron-based alloy which has similar mechanical properties to stainless steel is slow [114]. The iron-based alloy IFI remains in the body for a long time after fracture healing [115]. And iron tends to be stable in the human body, the degradation of iron-based alloy IFI may cause metabolic complications [116]. In addition, the magnetism of iron may interfere with the use of medical imaging equipment, such as magnetic resonance imaging. At present, the material matrix and its surface are treated by a variety of manufacturing technologies such as casting, electroforming and 3D printing, to achieve a faster degradation rate and reduce interference to medical imaging equipment [117].

The mechanical properties and degradation rate of zinc-based alloy can be adjusted by adjusting the proportion of different elements. But there are few studies on the mechanical dynamic stability of zinc-based alloy in the degradation process in human body. And there is a lack of consistent and repeatable experimental protocol standards for the evaluation of the biodegradability and compatibility of zinc-based alloy, so it is rarely used in clinical practice [118,119].

The use of degradable metals can make the structural stiffness of IFI change in the time dimension. The mechanical properties and degradation characteristics of different biodegradable metals are the main consideration factors for selecting them in different application ranges.

4.1.3. Shape memory alloy

With the unique crystalline structure, shape memory alloy can realize large deformations at low temperatures and restore their original shapes at a certain temperature. Shape memory alloy has been effectively used in the biomedical field in recent years due to good corrosion resistance, bending resistance, biocompatibility and magnetic resonance compatibility [120]. However, shape memory alloy itself has defects such as damage and crack, and its manufacturing and processing are difficult and costly.

4.1.4. Porous functional material

The porous functional material is a network structure composed of interconnected microstructural cells, and the relative stiffness of the porous material can be changed by adjusting the porosity. Titanium and tantalum are the most used porous functional materials for IFI due to their excellent mechanical properties and good biocompatibility [93]. By using porous functional material, the IFI with similar structure and mechanical characteristics to natural bone can be designed [121,122]. With the development of additive manufacturing technology, IFI with porous structures is more convenient to manufacture and able to meet the requirements of complex geometry and small dimension. But the loss of elements and porosity during additive manufacturing are still common issues, and there is less research on the effects of porous structures on cell biology [123,124].

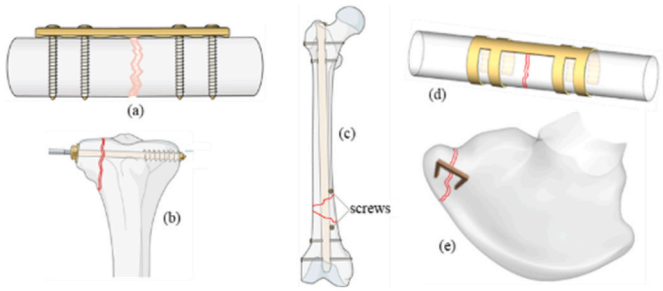

Fig. 10. Common IFI: (a) Bone plate, (b) Intramedullary nail, (c) Screw, (d) Embracing device, (e) Bone nail [3]. Copyright by AO Foundation, Switzerland.

4.2. Bioceramic

Bioceramic has good corrosion resistance and biocompatibility, but high brittleness, poor fracture toughness and poor manufacturability [95]. Bioceramic can be divided into two categories according to the response of active tissues to material: (1) Bioinert ceramic, such as zirconia and alumina; (2) Degradable bioactive ceramic, such as calcium phosphate ceramics. Pure ceramic is not suitable for IFI due to its poor mechanical properties, it is mostly used for bone defect fillers, bone scaffolds, false teeth, etc. [94]. Recently, high-performance ceramics have been manufactured by improving the raw material preparation and post-processing technology during additive manufacturing. Thus the potential application range of bioceramics is expanded [125].

4.3. Polymer composites

Pure polymer material is not suitable for IFI because of its poor mechanical properties. Relevant scholars have developed polymer composites by adding reinforcing materials to polymer [126–129]. Polymer composites can be divided into three categories: non-degradable, partially degradable and completely degradable. Polymer composites with different mechanical properties and degradation rates can be obtained by changing their composition and manufacturing methods to realize the function-oriented material design [89]. However, most of the current research on polymer materials is in laboratory stage. The lack of comprehensive research on mechanical and biological properties of polymer composites limited its clinical application [130].

To sum up, the materials currently used for IFI are mainly traditional metal supplemented by degradable materials, porous materials, shape memory alloys and other special functional metal materials. While bioceramics and polymer composites are rarely used. How to design materials with ideal mechanical and biological properties for IFI is still a challenge.

5. Design of IFI for fracture

When internal fixation is performed, appropriate IFI need to be selected according to the location and type of fractures. As shown in Fig. 10, common IFI include bone plate, intramedullary nail, screw,

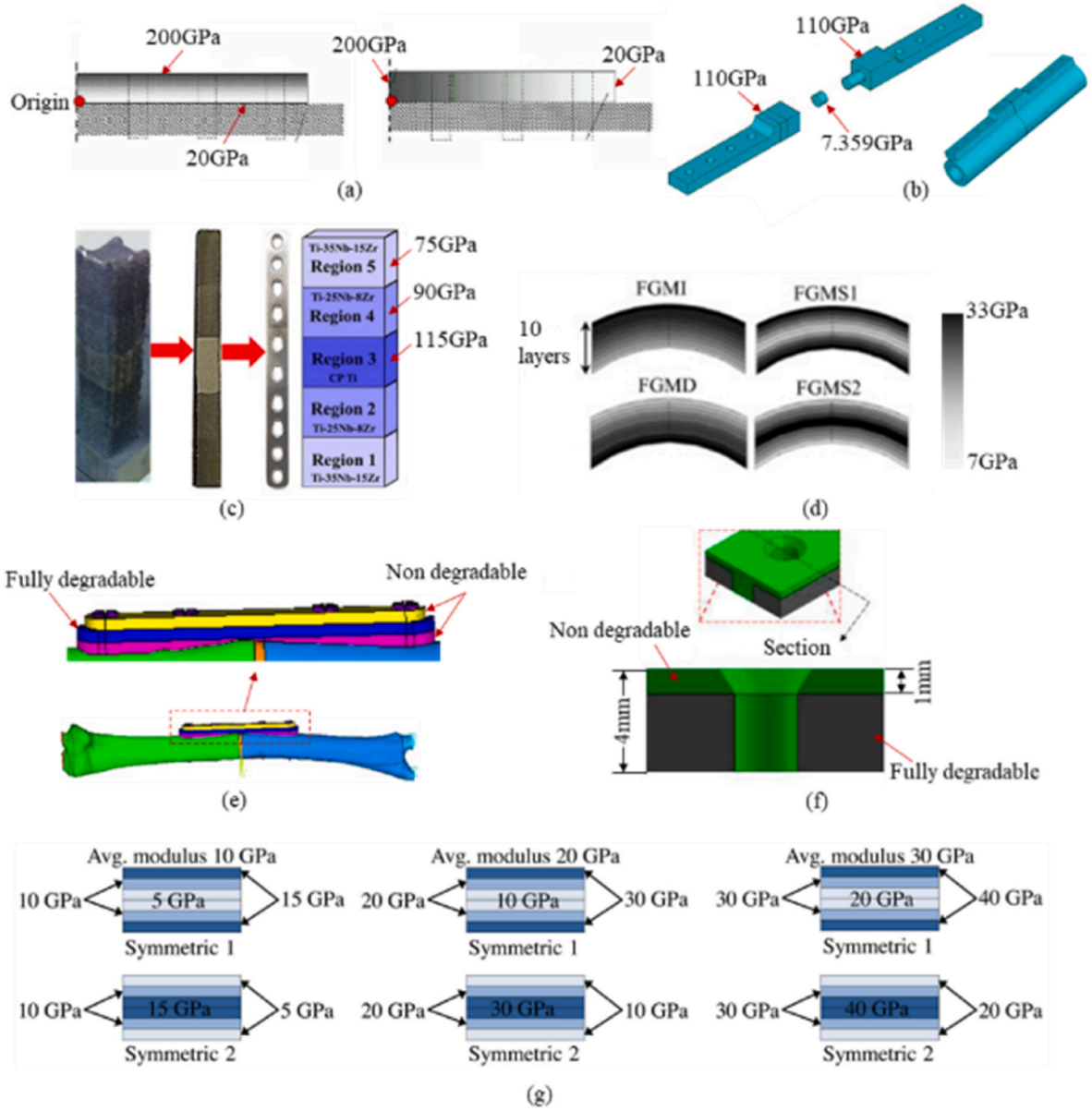

Fig. 11. The material based design of bone plates: (a) Functional gradient along thickness and length [45], (b) Plate with low-stiffness material [48], (c) Functional gradient plate and the additive manufacturing sample [142], (d) Plates with different functional gradient material composites [143], (e) Plate with biodegradable cushion [47], (f) Partially degradable plate [129], (g) Functional gradient biodegradable composite plates [146].

embracing device and bone nail. The fixation characteristics and application scope of different IFI are shown in.

Table 4.

As shown in Fig. 10(a), bone plate is a plate-like structure with holes and connected to the bone by screws. Different bone plates are designed according to the anatomical characteristics, fracture types and fixation needs of different bones. Bone plates have the widest application scope and are most used in clinical [131,132]. As shown in Fig. 10(b), the intramedullary nail is in the shape of a long rod with several screw holes at both ends and connected to fracture bone with screws. Intramedullary nail fixation is a stress dispersive fixation method which is not easy to produce stress shielding effect. It is applicable to the fixation of tubular long bone shaft fractures such as femur and tibia [133]. The fixation with screws alone is shown in Fig. 10(c). The incision of the surgery and the damage to soft tissue and bone tissue is small when only screw is used for fixation, but the fixation capacity is limited. It is suitable for the fixation of fracture with small bone fragments and large muscle traction, such as the medial and lateral condyles of femur and tibia, olecranon of ulna, tubercle of humerus and tubercle of tibia [9]. As shown in Fig. 10 (d), the embracing device utilizes the shape memory function of shape memory alloy to generate an embracing force, which does not require screw fixation and does not cause damage to the bones. Common shape memory IFI include patella grasper, carpal quadrangular cage, clavicle embracing device, phalangeal embracing device, rib embracing device, etc. [92,134]. The structure of bone nail is similar to that of staples, as shown in Fig. 10(e). The size of bone nail is small, and it is easy to implant and suitable for the fracture fixation of irregular bone such as condyle, acetabulum, and elbow [135].

5.1. Bone plate

The bone plate is most commonly used in clinical with excellent fixation stability and wide applicability. The bone plate is usually designed according to the anatomical morphology and load-bearing characteristics of fracture bone. Table 5 summarizes the existing bone plate design research from two aspects: design factors and design

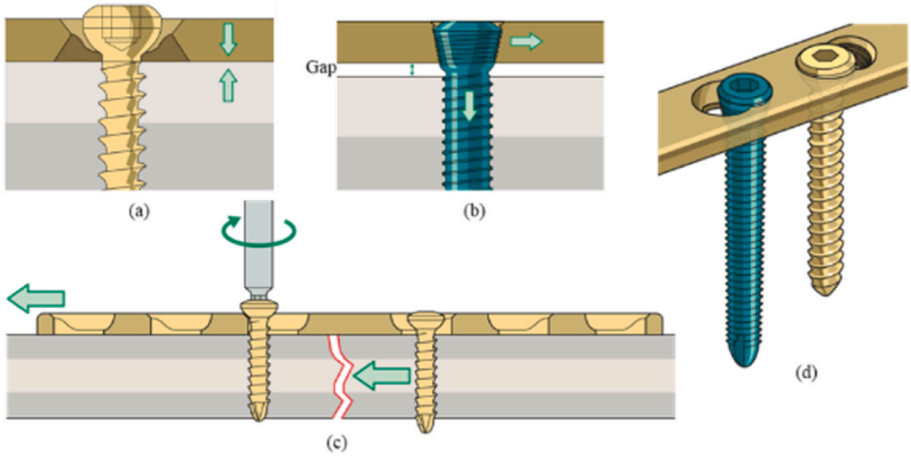

Fig. 12. Plates with different screw holes [168]: (a) Conventional plate, (b) Locking plate [165], (c) Dynamic compression plate [8], (d) Locking compression plate [166,167].

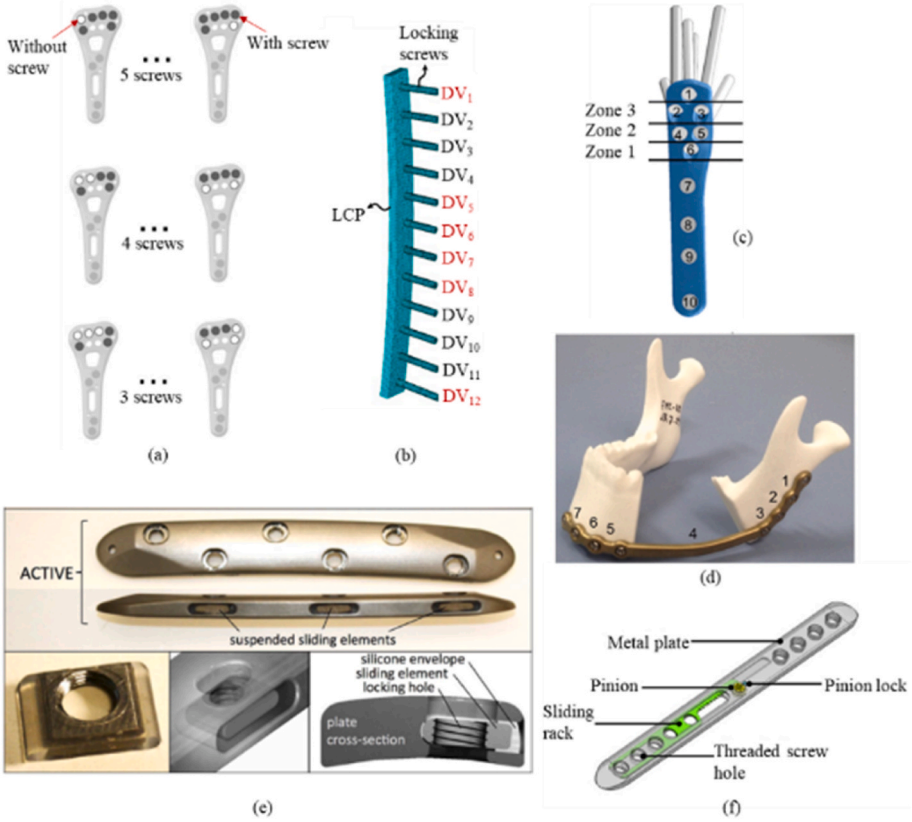

Fig. 13. Plate design based on screw type and layout: (a) Comparison design of screw layout of distal radius plate [147], (b) Optimization of the screw layout of femoral plate [51], (c) Optimization of the screw layout of proximal humerus plate [149], (d) Customized mandibular reconstruction plate [41], (e) Active plate with elastically suspended screw holes [131], (f)Adjustable locking plate [148].

methods. The design factors mainly include material type, screw layout and geometry structure. The design methods are comparative design and optimization design. The existing studies are described in detail below according to different design factors.

5.1.1. *Material based design*

The first step of design is to select suitable material, and Section 4 has introduced the commonly used biomaterials. With the development of material science and manufacturing technology, the variety of biomaterial is increased and the biomaterial is endowed with designability. It provides great convenience for the design of the bone plate based on material.

Nurettin et al. [44] and Murakami et al. [136] designed bone plate with carbon fiber-reinforced PEEK and PLA, respectively. Kim et al. [138,139] studied the effect of bone plates with different elastic modulus on fracture healing. The results showed that when the elastic modulus of bone plate is between 3 GPa and 70 GPa, the stress shielding effect can be alleviated and the fracture healing efficiency can be improved. Subsequently, the research of Zaheer et al. [140] showed that the best fracture healing performance can be obtained when the elastic

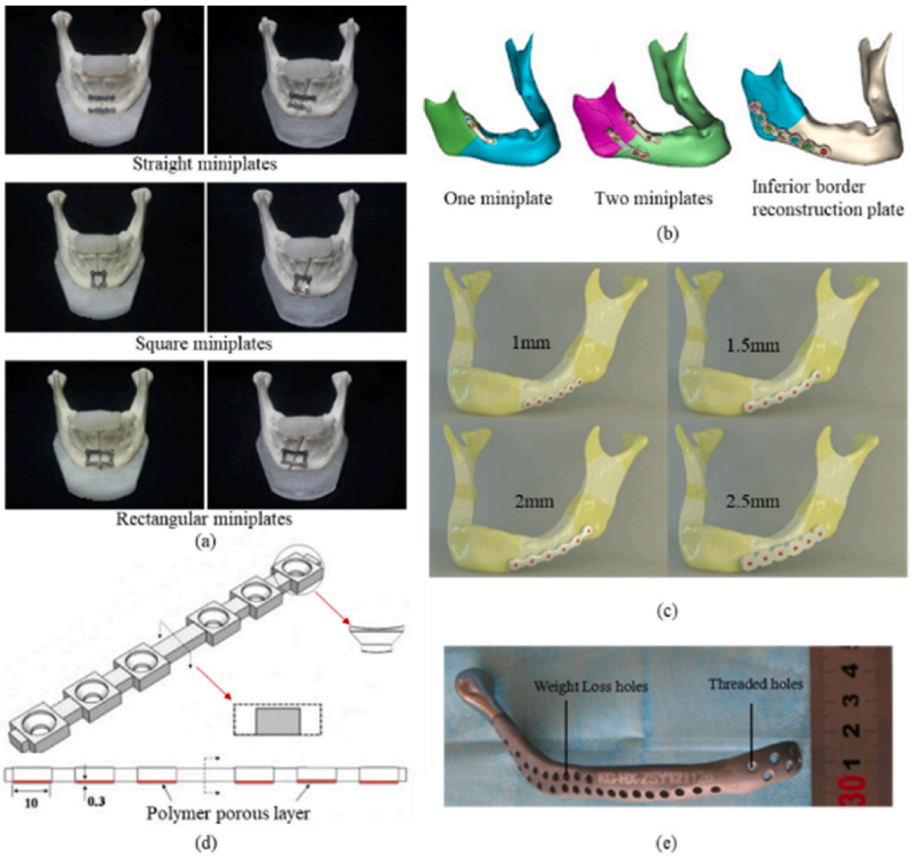

Fig. 14. Design of the plate structure: (a) Straight, square and rectangular miniplates [151], (b) Miniplates and inferior border reconstruction plate [43], (c) Mandible profile reconstruction plates with different thickness [44], (d) Variable cross-section plate with polymer porous layer [139], (e) Design optimization of customized mandible plate [152].

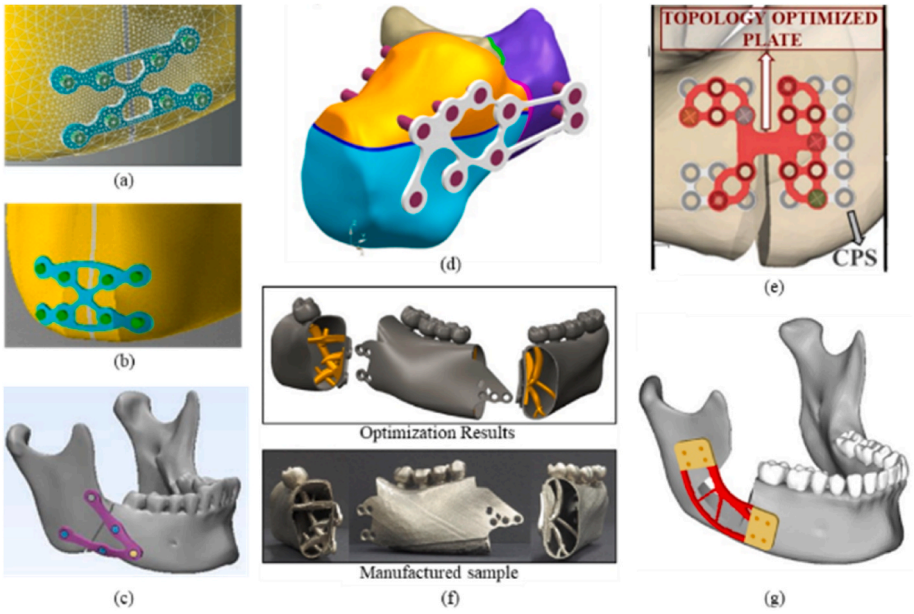

Fig. 15. Topology optimization of bone plate: (a) Plate for mandibular fracture [153], (b) Plate for mandibular symphysis fracture [154], (c) Mandible profile reconstruction plate [156], (d) Plate for intraarticular calcaneal fracture [159], (e) Topology optimization of plate based on screw hole distribution [157], (f) Integrated weighted topology optimization of patient-specific mandible reconstruction implant [155], (g) Time-dependent topology optimization of plate considering bone remodeling [158].

Table 4
Fixation characteristics and application scope of different IFI.

Type	Characteristics	Application Scope
Bone plate [131]	Eccentric fixation, it is fitted with bone and connected to bone with screws.	Simple fracture of most bones.
Intramedullary nail [133]	Central fixation, it is placed in the medullary cavity, and connected to bone with screws.	Diaphyseal fracture of long tubular bones.
Screw [9]	The incision is small, but the fixation capacity is limited.	Condyle, ankle, tuberosity or tubercle tear fracture; spiral, long oblique and butterfly fracture of long bones.
Embracing device [92,134]	The constant embracing force is generated by the shape memory property.	Comminuted fracture of the kneecap, diaphysis fracture of long bones.
Bone nail [135]	Similar in structure to staple, shape memory nails can provide active compressive force.	Fracture of irregular bone such as condyle, acetabulum, elbow, etc.

Table 5
Design of bone plate.

Design factor	Design method	Design case
Material type	Comparative design	Composite bone plate [12,44,136,137], Bone plate design with elastic modulus as design variable [138–141], Stiffness gradient bone plate [45,48,142,143](Fig. 11(a)–(d)), Bone plate with degradable layer [47] (Fig. 11(e)), Partially degradable bone plate [129] (Fig. 11(f)), Bone plate design with degradation rate design variable [144]
	Optimization design	Reinforced composite bone plate [52], Bone plate with auxetic structure [145], Degradable bone plate with stiffness gradient in thickness direction [146] (Fig. 11(g))
Screw layout	Comparative design	Plate for long bone [39](Fig. 13(a)), Plate for distal radius [147] (Fig. 13(b)), Dynamic locking bone plate [131](Fig. 13(f)), Bone plate with adjustable screw hole [148] (Fig. 13(g))
	Optimization design	Plate for long bone [51] (Fig. 13(c)), Humerus plate [149] (Fig. 13(d)), Mandible bone plate [41] (Fig. 13(e))
Geometry structure	Comparative design	Type X, L, T and I mandibular plate [150], Long, square and rectangular mandibular plate [151] (Fig. 14(a)), Bone plate design with bone anatomy as the initial structure [43] (Fig. 14(b)), Bone plate design with thickness as design variable [44] (Fig. 14(c)), Variable rectangular cross-section bone plate [139] (Fig. 14(e))
	Optimization design	Mandibular plate: Parameter optimization design [152] (Fig. 14(e)), Topology optimization design [153,154] (Fig. 15(a) and (b)), Topology optimization design of bone for comminuted fracture [155](Fig. 15(f)), Topology optimization design based on the structure fitted to the morphology of bone dissection as the initial design domain [156] (Fig. 15(c)), Step-by-step optimization design of screw layout and structure [157] (Fig. 15(e)), Topology optimization design considering bone remodeling [158](Fig. 15(g)); Topological optimization design of calcaneal plate [159] (Fig. 15(d)); Topological optimization design of bone plate considering different loading conditions [160–163]

modulus of bone plate is 40 GPa under certain conditions. Son et al. [141] studied the influence of the elastic modulus of bone plate on the healing performance under different fracture angles and initial load conditions, and proposed the reference value of the optimal elastic modulus of bone plate for different fracture situations. In addition, Son et al. [164] studied the bone healing performance of fractured long bones applied with a composite bone plate with consideration of the blood vessel growth. The results show that the effect of the plate modulus on the healing performance reduced when the blood vessel growth at the fracture site was considered, which reflected a more realistic bone healing process. Samiezadeh et al. [52] calculated the axial stiffness, bending stiffness and torsional stiffness of bone plate in fixed state according to the classical lamination theory and the composite beam theory. With the maximum bending and torsional stiffness and the minimum axial stiffness as the optimization objectives and the stacking order of composites as design variables, the reinforced composite bone plate was optimized. The results showed that compared with the traditional metal bone plate, the compression force at the fracture site increases by 14 % when using the bone plate with axial stiffness, bending stiffness and torsional stiffness of 4.6 MN, 13 $N{\cdot}m^2$ and 14 $N{\cdot}m^2$ respectively. Based on the designability of microstructure, Vijayavenkataraman et al. [145] designed a bone plate with auxetic structures which is located in the central area of bone plate. The bone plate with auxetic structures can not only effectively reduce the stress shielding effect, but also meet different clinical needs through adjusting the bending of plate.

Some scholars believed that the stiffness gradient bone plate can reduce the stress shielding effect, and had carried out relevant research. As shown in Fig. 11 (a), Ganesh et al. [45] studied the effect of functional gradient along the length direction and the thickness direction on the stress distribution of the bone–bone plate system, respectively. The results showed that the functional gradient bone plate can reduce the stress shielding effect to a certain extent in different healing periods compared with stainless steel bone plate. Benli et al. [48] designed a segmented functional gradient bone plate, as shown in Fig. 11(b), using two materials with different elastic modulus. Using additive manufacturing technology and titanium alloys with different elastic modulus, Lima et al. [142] designed and manufactured a functional gradient bone plate, as shown in Fig. 11(c). Mehboob et al. [143] designed functional gradient bone plates using composites, as shown in Fig. 11(d). The bone plates have same equivalent elastic modulus and different functional gradient along the thickness direction. The healing rate when using the FSMS2 bone plates, as shown in Fig. 11(d), is highest and higher than that when using homogeneous bone plates.

The use of degradable materials can make the structural stiffness of bone plate gradually reduce in the fracture healing process, and betterly meet the biomechanical requirements at different fracture healing stages. As shown in Fig. 11(e), Fan et al. [47] added a degradation layer in the bone plate. The finite element analysis and animal experimental results showed that the bone plate with the degradation layer can meet the requirements of fixation stability at the initial stage of fracture healing. With the degradation of the degradation layer, the stress shielding effect is effectively alleviated at the later stage of healing and good blood supply is maintained. Mehboob et al. [129] designed a partially degradable bone plate as shown in Fig. 11(f). The healing rate of fixation with the partially degradable bone plate is more than twice of that with stainless steel plate of the same structure. Subsequently, Mehboob et al. [144] proposed the appropriate degradation rate of bone plate materials for different fracture angles and fracture gaps to obtain the best healing effect. After that, Mehboob et al. [146] designed the biodegradable functional gradient bone plates. As shown in Fig. 11(g), the average elastic modulus, functional gradient sequence, material degradation rate and plate thickness were taken as design variables. The Taguchi method was used to determine the optimal level of design parameters with the maximum fracture healing rate as the optimization objective.

5.1.2. Design of screw type and layout

Screws are usually used to connect the bone plate to the fractured

bone. The traditional plate is shown in Fig. 12(a), the stability is maintained by the friction between bone and bone plate. But the excessive pressure on the bone from the bone plate may damage periosteum and blood supply. Tepic et al. [165] designed a locking screw hole as shown in Fig. 12(b), the stability of the bone plate depends on the stable coupling between the screw head and the plate hole. There is a certain gap between bone plate and bone to reduce the destruction of periosteum and blood supply. To provide axial compression on the fracture site, Perren et al. [8] designed a dynamic compression plate as shown in Fig. 12(c). Combining the advantages of locking plate and dynamic compression plate, Sommerd et al. [166,167] designed a locking compression plate, which is the most common bone plate type at present. As shown in Fig. 12(d), locking or compression screws is used.

The bone needs to be drilled before implanting screws, the number and position of implanted screws have a great influence on the fixation stability. To reduce the number of implanted screws on the premise of meeting the requirements of fixation stability, relevant scholars have studied the design of screw layout. The distance between the two screws closest to the fracture site on either sides is called the bridging length. Stoffel et al. [39] replaced bone with a homogeneous composite circular tube, and found that the bridge length is the main reason affecting the axial stiffness and torsional stiffness of the bone–bone plate system by using the combination method of simulation and experiment. As shown in Fig. 13(a), Synek et al. [147] designed 41 screw layouts for the distal radius bone plate, with axial stiffness as the constraint and the minimum strain of the bone surrounding the implanted screw as design objective, the screw placement for the specific fracture condition was optimized. As shown in Fig. 13(b), Lee et al. [51] established models of the femoral fracture and the 12-hole plate. The minimum of the maximum displacement of femoral-plate system was set to be optimization objective and the presence or absence of screws was set as design variables. The total number of implanted screws and the number of screws implanted at either side of fracture site were set as constraints. Particle swarm optimization algorithm was used to get the best screw layout of 1-5-6-7-8-12, and the optimization result was verified by mechanical tests using synthetic plastic fiber femur. Jabran et al. [149] used the artificial humerus and characterized the fixation stability by the displacement between the fracture site under loading. Through the sensitivity analysis of mechanical experiments, it was determined that the screw in Zone 2, as shown in Fig. 13(c), has the greatest influence on the fixation stability. Then the angles of the screws in Zone 2 to the horizontal and vertical directions were taken as the design variables. The optimal screw implantation directions were determined with the optimal fixation stability as the optimization objective. Gutwald et al. [41] used the finite element method to optimize the mandibular bone plate with the distance between the screw holes as design variables and the minimum of the maximum stress of bone plate as optimization objective. The optimization results were shown in Fig. 13(d), the maximum stress on the optimized plate is reduced by 31 % compared to the standard plate. Bottling et al. [131] designed a dynamic locking plate, as shown in Fig. 13(e), which was the same size as a standard locking plate. The screw hole component is located in the silicone sleeve to achieve limited sliding, and the bone–bone plate system can achieve dynamic stability. For segmental fractures, Subasi et al. [148] designed a bone plate with adjustable screw hole, as shown in Fig. 13(f), which could achieve the function of compression, traction or segmental transfer of broken bone by using the pinion mechanism with adjustable rack.

The design variables of bone plate from the perspective of screw layout mainly include the position, number and implantation angle of the screws. The study of the impact of screw layout on fracture healing not only can guide bone plate design but also can provide references for doctors in clinical.

5.1.3. Geometric structure design

The structure of the bone plate has very important influence on its overall stiffness. By designing the structure of bone plate, it can better meet the biomechanical requirements of fracture healing. In the structure design of bone plate, the comparative design of single design variable with the mechanical properties of bone plate as design goal was mainly used at the beginning. Later, it developed to the comprehensive optimization design with multiple design variables and the optimization design based on fracture healing theory.

Korkmaz et al. [150] designed X-shaped, L-shaped, T-shaped and I-shaped mandibular plates, and analyzed the effects of different types of plates on fixation stability by finite element method. The results showed that X-shaped plate can provide the best fixation stability. Oliveira et al. [151] designed some long, square and rectangular mandibular plates, as shown in Fig. 14(a), and analyzed the stability of the bone–bone plate system through mechanical tests. The results showed that the stability with rectangular plates was the best. As shown in Fig. 14(b), Wang et al. [43] compared the stress and strain distribution of the bone–bone plate system when the mandible fracture was fixed with one miniature bone plate, two miniature bone plates and bone plate designed according to bone anatomy, respectively. The results indicated that the best fixation effect was achieved when using two miniature plate. Nurettin et al. [44] analyzed and compared the distribution of stress and displacement of the bone–bone plate system when using mandibular plates with different thicknesses as shown in Fig. 14(c). And the results reflected that the plate with thickness of 2 mm was more suitable for clinical use. Using polymer materials, Kim et al. [139] designed a variable rectangular cross-section bone plate with porous layer as shown in Fig. 14(d). When using the cross-section bone plate, the reasonable mechanical stimulation could be produced on fracture site and the contact stress in the contact area of bone and bone plate was effectively reduced. The above designs of bone plate structure is only based on experience to adjust the macrostructure of bone plate through comparison, and the design result is not optimal. Qin et al. [152] optimized the mandibular bone plate with the transition fillet radius, cross-section type and screw distribution as design variables and structural strength as optimization objective. The design result is shown in Fig. 14(e).

The topology optimization method is an effective structural optimization design method, which can determine the optimal distribution of materials in the design domain according to the given load, constraint conditions and optimization objectives. Aiming at the lateral fracture and centerline fracture of the mandible, Lovald et al. [153,154] designed an eight-hole rectangular solid titanium plate with the maximum stiffness of bone plate as the optimization objective and the volume fraction as constraints by using SIMP (Solid Isotropic Material with Penalization) method. Then the parameters such as the radius of the fillet, the thickness and the distance between the screw holes were optimized, and the design results are shown in Fig. 15(a) and (b), respectively. Liu et al. [156] established the finite element model of the mandible with 1 mm fracture gap, the structure fitted to the anatomy morphology of the bone was taken as the design domain. And the volume constraints and displacement constraints were set. The V-shaped plate, as shown in Fig. 15(c), was obtained through topology optimization with the maximum structural stiffness as the optimization objective. As shown in Fig. 15(d), Ouyang et al. [159] designed a new type of bone plate for saunders type II-C calcaneal fracture by using topology optimization. Al-Tamimi et al. [160–163] performed topology optimization of long bone plates under different loading regimes. For the mandible bone plate, Sensoy et al. [157] first used the particle swarm optimization algorithm to optimize the screw distribution. And then the topology optimization of structure was carried out according to the optimized screw distribution position. The design result is shown as the red structure in Fig. 15(e). As shown in Fig. 15(f), Li et al. [155] adopted the step-by-step optimization method to optimize the design of the IFI for comminuted fracture of the mandible. Firstly, the topology optimization of the fixed wings at both ends of IFI was carried out. And then the main structure of IFI was optimized by considering the weighting effects of axial and oblique loads. Finally, the design result was manufactured

Table 6
The design of intramedullary nails.

Design factor	Design case	Character
Material type	Conventional type [21, 173–175]	Titanium alloy, stainless steel or composite material are used.
	Active compression type [92,176](Fig. 16(e))	The pseudoelasticity of Ni-Ti alloy is used to produce active axial compression.
Screw type	Locking screw [177,178] (Fig. 16(a))	Apply axial pressure by striking the impact plate
	Dynamic screw [179] (Fig. 16(b) and (c))	The stiffness of the fixation system is reduced by removing the dynamic screw in the middle of bone healing,
	Axial compression screw [180] (Fig. 16(d))	Axial pressure is applied by adjusting the axial screw.
Geometric structure	Medullary cavity matching [181](Fig. 17 (a))	The intramedullary nail is designed by quantifying the curvature of medullary cavity.
	For complex femoral shaft fracture [182](Fig. 17(b))	The nail is perforated and the Kirschner wire is used to fix the fracture block.
	Multiple section expandable [183] (Fig. 17(c))	Without screw fixation, the self-locking function is realized by pressing the expansion unit against the medullary wall.
	Elastic self-locking [184] (Fig. 17(d)–(f))	Without screw fixation, the self-locking is realized by elastic rods.

by additive manufacturing technology and mechanical experiments were carried out. All of the above topology optimization designs used the maximum stiffness of bone plate as optimization objective, which can make the bone plates have good mechanical properties, but may not guarantee the mechanical environment required for fracture healing. Wu et al. [158] proposed a bone plate topology optimization method considering bone remodeling. Using the SIMP method, the maximum bone density in the final stage of bone remodeling was taken as the optimization objective. The optimization result with 40 % the volume fraction is shown in Fig. 15(g). Using two kinds of biodegradable materials with different material properties, Zhang et al. [169–171] proposed a topology optimization design method for biodegradable composite structures considering time-changing stiffness characteristic. After that, Zhang et al. [172] designed a biodegradable bone plate, in which the time-changing stiffness characteristic of plate was regulated according to the changing biomechanical requirements in fracture healing process.

In summary, the existing research of bone plate design is introduced from the perspective of design factors. Although the design of bone plate has made great progress, there are still some problems remained. The mechanical response is still mainly used as the evaluation indexes or optimization objective and the design based on the fracture healing theory is less. In addition, there is no cooperative design of bone plate structure, screw layout and other related design factors.

5.2. Intramedullary nail

The design factors of intramedullary nail mainly include material type, screw hole type, radius of curvature and fixation form. The existing design of intramedullary nail is summarized according to different design variables in Table 6. Gabarre et al. [173] used finite element

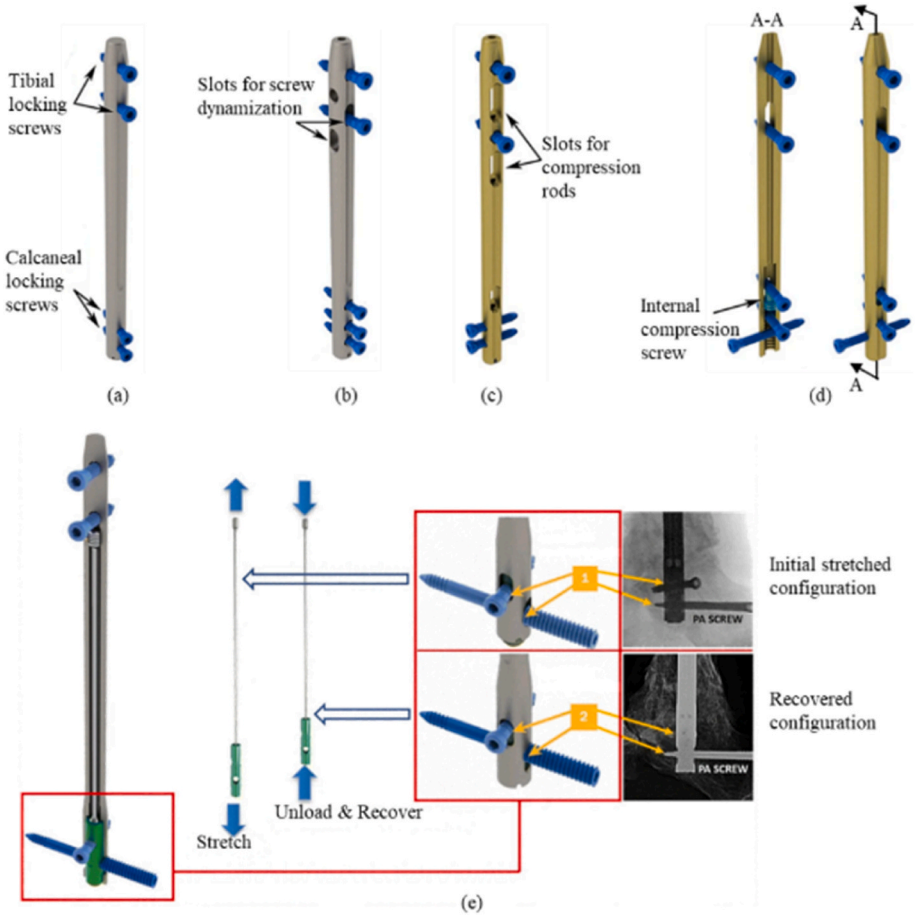

Fig. 16. Different types of intramedullary nails: (a) Traditional nail with locking screws in holes [177,178], (b) and (c) Nail include slots for compression and screw dynamization [179], (d) Nail include internal compression screw and slots for screw dynamization [180], (e) Nail incorporating pseudoelastic NiTiNOL element [92,176].

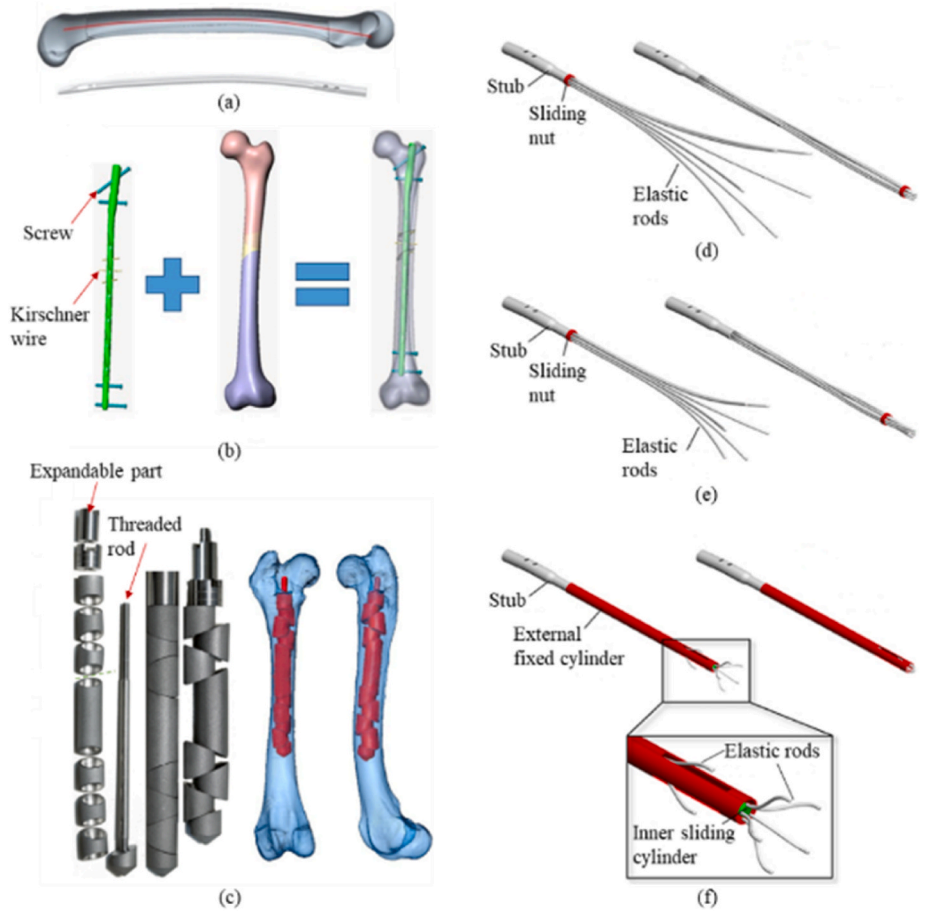

Fig. 17. The design of intramedullary nail: (a) Designed to match the curvature of the femur [181], (b) Nail with grooved for Kirschner wire [182], (c) Expandable intramedullary nail [183], Elastic self-locking nail [184]: (d) Traditional, (e) Revised version, (f) Terzini-Putame

method to analyze and compare the biomechanical environment on fracture site when using stainless steel intramedullary nail and titanium alloy intramedullary nail for femoral shaft fracture. Mehboob et al. [21,174] studied the effect of elastic modulus of intramedullary nail on tibial fracture healing with different fracture gap and angle. And the best elastic modulus of intramedullary nail for different fracture conditions were proposed.

As shown in Fig. 16(a), the traditional intramedullary nail is connected to the bone by locking screws, and the compression force is applied to the fracture site by hitting the impact plate [177,178]. The improved intramedullary nails, as shown in Fig. 16(b) and (c), have slots for dynamic screws and compression rods, respectively. It is convenient to apply axial compression to the fractured bone during operation [179]. As shown in Fig. 16(d), Karakasli et al. [180] designed an intramedullary nail with compression function by setting internal compression screws. The structure property of the above intramedullary nails is static and it cannot provide active pressure continuously. Although the fixation stiffness can be reduced by removing dynamic screws, a second operation is needed. The active compression intramedullary nail designed using the pseudo elasticity of Ni-Ti shape memory alloy is shown in Fig. 16(e). The Ni-Ti unit is in stretch state when the intramedullary nail is implanted into medullary cavity. Then it recovers to normal state without load [92,176].

When using intramedullary nail for fixation, it is necessary to adjust the curvature of intramedullary nail to match the medullary cavity. Arnone et al. [181] scanned 40 complete adult femurs and established an average geometric model using CT data. As shown in Fig. 17(a), the intramedullary nail matching the actual geometric shape of the medullary cavity was designed by quantifying the curvature of the medullary

Table 7
The design and characteristics of smart IFI.

Type	Design case
Bone nail	OSStaple [185](Fig. 18(a)), thermally activated OSSatple, Room temperature hyperelastic EasyClip and Body temperature shape memory BioPro [186] (Fig. 18(b) and (c)), Arched bone nail with a tooth-like structure [187] (Fig. 18(d)), Different sizes of arched bone nails [135] (Fig. 18(e)), Acetabular Shape Memory Fracture Implant System [188] (Fig. 18(g))
Connector	Olecranon shape memory connector [189](Fig. 19(a))
Embracing device	Patella claw [190] (Fig. 19(b)),Embracing device with serrations [191] (Fig. 19(c)),Parameter optimization design of embracing device [192] (Fig. 19(d)),Swan-like embracing device [193–196] (Fig. 19(e))

cavity. For some complex femoral shaft fractures, Cui et al. [182] made holes in the nail body and fixed the fracture block with Kirschner wire, as shown in Fig. 17(b). To provide sufficient fixation stability without screw fixation, Plenert et al. [183] designed a multi-segment expandable intramedullary nail, as shown in Fig. 17(c). It is implanted into the medullary cavity in the initial state, and the self-locking function is realized by pressing the expansion unit against the medullary wall. As shown in Fig. 17(d), the Marchetti-Vicenzi elastic self-locking intramedullary nail is composed of six elastic rods which are kept closed by a sliding nut. And the elastic rods are stretched freely by moving the nut after implantation. Putame et al. [184] first designed the improved Marchetti-Vicenzi intramedullary nail, as shown in Fig. 17(e), by reducing the length and bending radius of the elastic rod. And then a new type of Terzini-Putame elastic self-locking intramedullary nail with

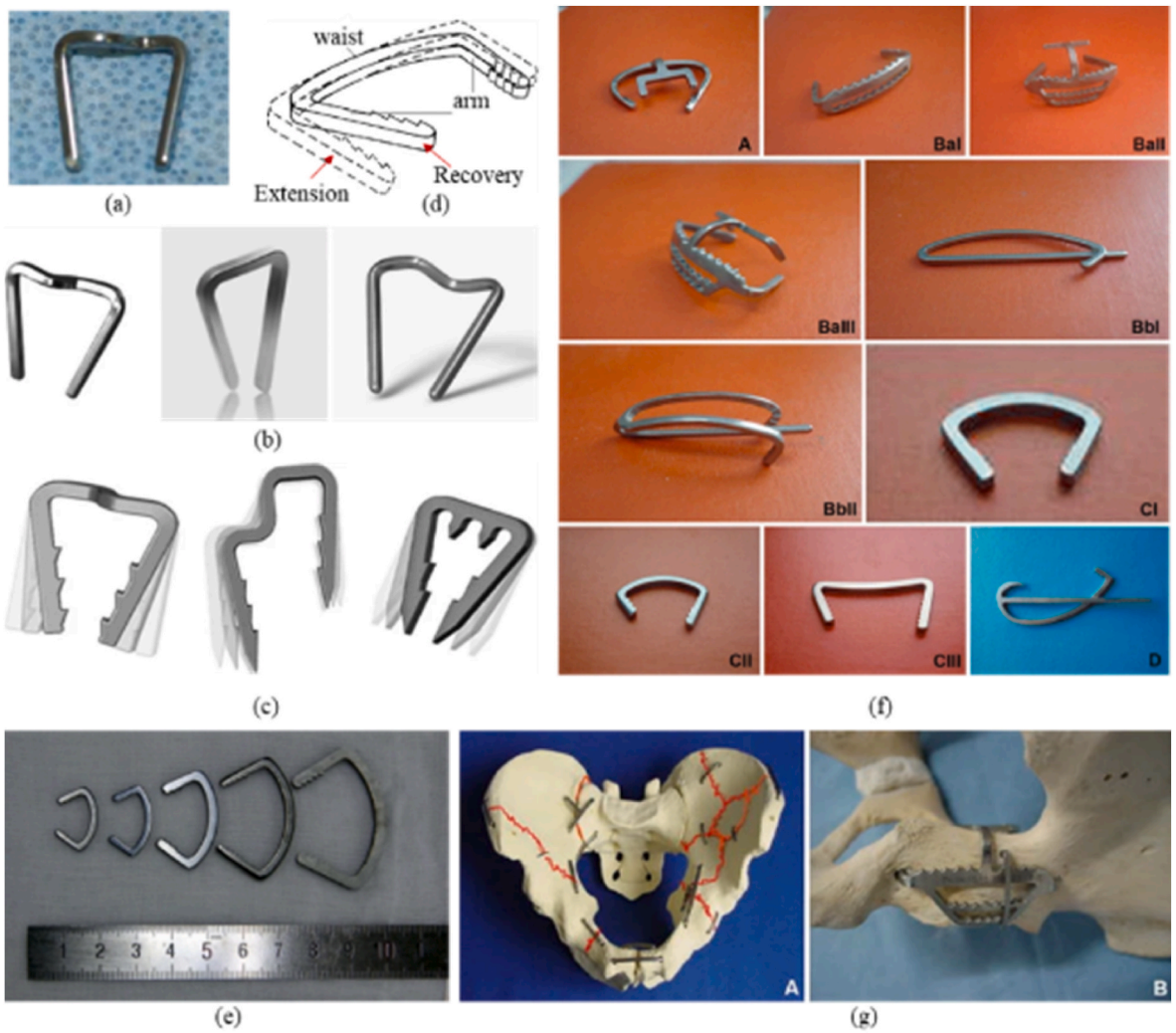

Fig. 18. The design of Nitinol bone staple: (a) OSStaple [185], (b) Commercially available Nitinol bone staples [186], (c) Barbed OSStaple [186], (d) Arched bone staple [187], (e) Arched bone staple of different sizes [135], (f) Acetabular tridimensional memory alloy-fixation system (ATMFS) device of four series [188], (g) Working principle of the ATMFS device [188].

distal and proximal elastic rods was designed, as shown in Fig. 17(f).

The elastic self-locking intramedullary nail does not need to implant screws which can avoid secondary injury to the bone, and sufficient fixation stability can be provided. However, most of the existing designs of intramedullary nail are comparative designs that may not reach the optimal structures.

5.3. Smart IFI based on shape memory alloy

The smart IFI based on shape memory alloy mainly include bone nail and embracing device, the existing designs are summarized in Table 7. Shibuya et al. [185] verified that the uniform compression force can produce at fracture site by using OSStaple bone nail, as shown in Fig. 18 (a). Russell et al. [186] introduced the thermally activated OSStaple, room temperature hyperelastic EasyClip bone nail and body temperature shape memory BioPro bone nail from left to right in Fig. 16 (b). And the design ideas of bone nail with hook structure, as shown in Fig. 18(c), were put forward [186]. As shown in Fig. 18(d), Cao et al. [187] designed an arched bone nail with a tooth-like structure. And the clinical results showed that the use of this bone nail can effectively improve fracture healing efficiency. As shown in Fig. 18(e), Zhang et al. [135] designed different sizes of arched bone nails with hook-like structures. Based on the anatomical morphology and biomechanical characteristics of the acetabulum, Liu et al. [188] designed a set of acetabular smart IFI using Ni-Ti alloy, as shown in Fig. 18(f), and the fixation effect is shown in Fig. 18(g).

Chen et al. [189] designed an olecranon shape memory connector for elbow fractures, as shown in Fig. 19(a). For patella fractures, Liu et al. [190] designed a patella claw, as shown in Fig. 19(b). As shown in Fig. 19(c), Li et al. [191] added serrations to the arms of the embracing device to prevent the fracture fragments from loosening. As shown in Fig. 19(d), Ko et al. [192] optimized the design of the embracing device with the contact pressure between the embracing device and the bone as the optimization objective and the circumference angle, thickness and inner diameter of the embracing device as design variables. As shown in Fig. 19(e), Zhang et al. [193–196] designed a swan-like embracing device that can provide axial pressure actively to the fracture site. And the clinical treatment effect of humerus, ulna, radius, clavicle and other long bone shaft fractures was studied through clinical follow-up.

Smart IFI has been gradually used in the clinic because of its unique advantages. It is necessary to consider how to make the design results meet the requirements of fixation stability and take the appropriate active compression produced at fracture site in the design.

6. Additive manufacturing of IFI

When it comes to the fabrication of implants, there are generally two common methods employed: subtractive manufacturing and additive

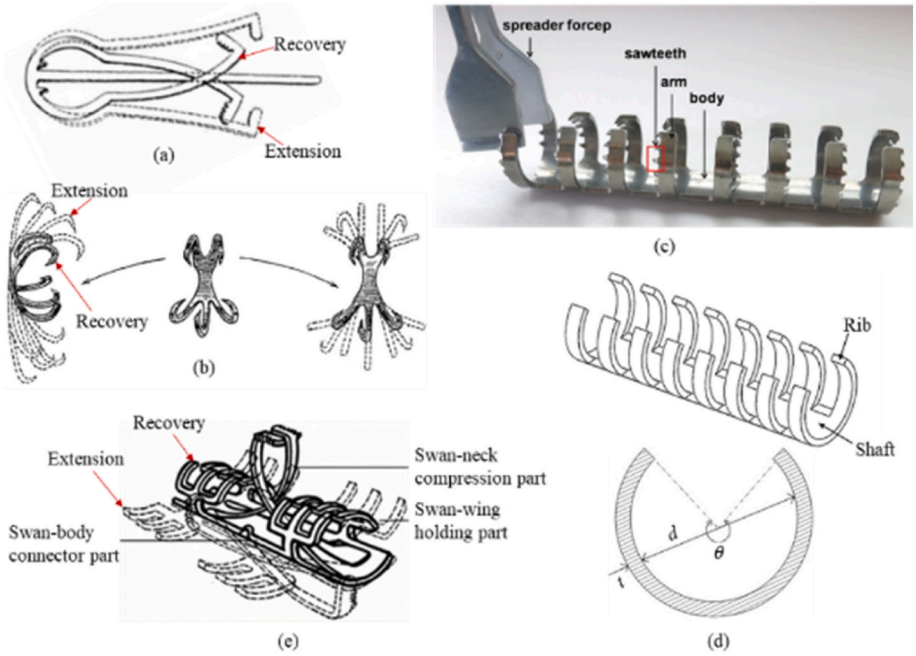

Fig. 19. Connector and Embracing device: (a) Olecranon memory connector [189], (b) Patellar shape-memorial fixator [190], (c) Sawtooth-arm embracing clamp [191], (d) Design optimization of embracing clamp [192], (e) Swan-like embracing clamp [193–196].

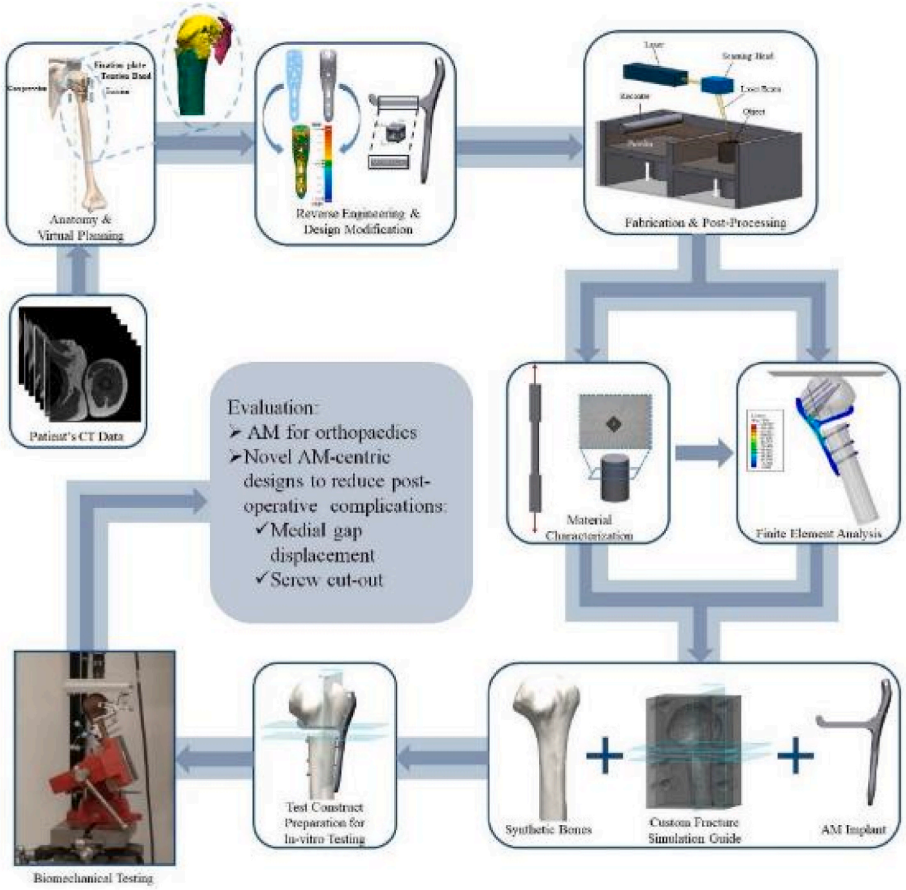

Fig. 20. Schematic diagram of the general workflow to evaluate AM for orthopaedic applications [199].

(1)Design

manufacturing (AM) processes. AM involves the layer-by-layer deposition of materials to build three-dimensional components. It has the advantage of rapidly and accurately producing metallic or non-metallic complex parts with a reasonable cost, which are unachievable through subtractive processes [197]. Thus motivate researchers to consider this fabrication technique as a revolutionary solution for patient-specific orthopaedic implant manufacture [198]. The typical steps involved in additive manufacturing (AM) procedures from conceptual design to the production of the final end-use IFI products can be divided into four main stages [199], as shown in Fig. 20.

The initial step involves designing the 3D models of the IFI for printing. Typically, computerized tomography (CT) or Magnetic Resonance Imaging (MRI) scanning techniques are utilized for visualization and to create the patient-specific medical models. This data is used to design a digital 3D model of the implant, which can be customized to fit the patient's anatomy precisely. Subsequently, Finite Element Analysis (FEA) is utilized to simulate the mechanical behavior of the designed implant under physiological loads. This helps in optimizing the design to ensure adequate strength and stability while minimizing the risk of failure.

(2) Manufacture and post-processing

Once the 3D model of the IFI device is designed, the second stage involves the actual printing process can be initiated. Before printing, a suitable material must be selected by considering the metrial properties, such as strength, flexibility, and biocompatibility, which influence the bone fracture healing. Once the material is selected, the printing process begins. The CAD model is first converted into a standard tessellation language (STL) file. The STL file is then sliced into thin horizontal layers, which will be printed layer-by-layer sequentially. The 3D printer reads the sliced STL file and begins manufactue. After printing, the object requires post-processing to achieve the desired finish and properties, including removing supporting structures, surface finishing, and heat treatment.

(3) In silico test

The CAD models of the bone fragments and the implants were assembled in the 3D modeling software, such as SolidWorks, UG and CATIA, to accurately simulate implantation. Then the assembled CAD model is imported into finite element software, such as Abauqs and Ansys, for FE modeling. The orthotropic material properties associated with the corresponding AM processing are obtained based on material characterization test. Different boundary conditions similar to the test constructs in experiments and physiological loads are modeled and solved to evaluated biomechanical performance of the IFI. The bone healing simulation model can also be used to predict the performance of AM implants.

(4) In-vitro and in vivo experiments

In vitro experiments are conducted to evaluate the biological and mechanical properties of AM implants. These experiments typically involve testing the implants in simulated body fluids to assess their corrosion resistance and biocompatibility. Mechanical testing, such as compression and fatigue tests, are also performed to ensure that the implants can withstand the forces they will encounter in the body. In vivo experiments are crucial for understanding the complex interactions within a whole, living system, which cannot be fully replicated in vitro. Before clinical trials the animal experiments can be used to study the in vivo performance of AM implants. These experiments provide critical data on the biological response to the implants. Clinical trials are the final step in the validation of AM implants. These trials involve implanting the devices in human patients and monitoring their performance over time. Long-term studies are also needed to fully understand the benefits and potential risks associated with these implants.

The human skeleton consists of two primary types of bone: trabecular and cortical (compact) bone. Trabecular bone, also known as cancellous bone, is characterized by a spongy structure with high porosity, which can reach up to 90 % [200]. In contrast, cortical bone is dense and compact, with a porosity ranging from 3 % to 5 %, which provides structural support and protection for the body. The distinct permeability and correlation required by each bone type are critical for their respective functions. For instance, the high porosity of trabecular bone is essential for metabolic processes, while the low porosity of cortical bone ensures strength and durability. In the context of medical implants, biocompatibility is a paramount consideration. An implant must not only be compatible with the body's biological environment but also possess the appropriate mechanical properties to function effectively. Micro open pores in the implant is crucial for bone regeneration, as these small pores provide the necessary surface area for cellular attachment and proliferation [201]. In orthopaedic applications, the average pore diameter used in implants typically ranges from 400 to 600 μm, with a volume porosity between 75 % and 85 %. This specific pore size and porosity range have been found to facilitate optimal tissue growth, cell attachment, and proliferation, thereby enhancing the overall success of the implant [202].

Implants must align their mechanical properties with human bones or tissues to ensure successful integration and functionality. Titanium and its alloys are commonly used biomaterials due to their biocompatibility and corrosion resistance [203], but they have a higher elastic modulus than bone, which will lead to stress-shielding effect. To mitigate this issue, researchers have developed porous titanium implants. The introduction of porosity reduces the overall stiffness of the implant, making it more comparable to natural bone. Innovative additive manufacturing techniques enable the fabrication of complex porous structures with high precision in both geometry and pore size distribution [204]. These structures can be tailored to improve specific properties, such as promoting bone growth, enhancing the integration of bone and implant, and reducing the implant's weight [205]. After the production process, permeable metallic frameworks often undergo surface modification or treatment procedures, which may include the application of bioactive substances or the integration of drug delivery systems to further enhance their mechanical and biological properties [206–208]. Orthopedic specialists use these structures to create porous implants, including bone scaffolds, hip replacements, and spinal fusion devices. These implants foster tissue regeneration and integration by providing an optimal environment [209]. The incorporation of porous metallic structures through additive manufacturing offers promising opportunities in orthopedic treatments, not only enhances the mechanical compatibility of the implant but also promotes bone ingrowth and osseointegration, further stabilizing the implant within the body [210].

Although AM is promising, it also has some limitations. AM process is not suitable for some specific application, for instance, the femoral head of hip implant must be smooth to facilitate joint movement and prevent erosion, the AM printed implants can not meet the required tolerance and surface finish specifications. Furthermore, the fabrication of 3D-printed scaffolds has several requirements to ensure success and widespread application. Collaboration between medical and engineering experts and familiarity with 3D bioengineering capabilities are crucial. The 3D printer should be compatible with biocompatible materials at an affordable cost. Biomaterial selection involves determining optimal combinations to achieve the desired functional, mechanical, and supportive properties [209]. The transition of research from laboratory experiments to practical clinical applications faces challenges stemming from technical, collaborative, and regulatory factors. In clinical applications, successful utilization of 3D printing demands expertise across diverse multidisciplinary domains. Clinicians collaborate with engineers or prosthetists to design patient-specific implants based on scans, while the pharmacy handles implant packaging and sterilization.

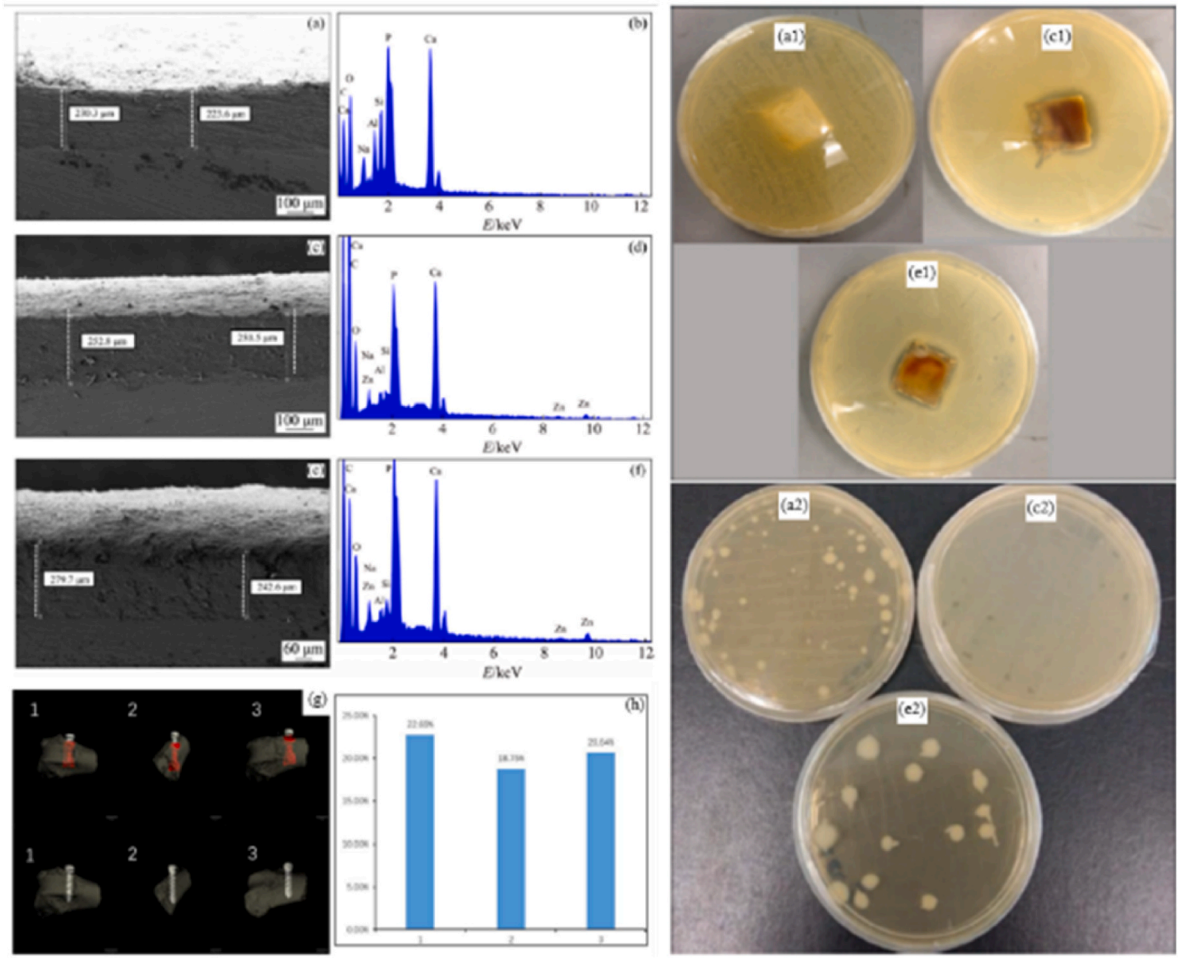

Fig. 21. Cross-sectional FESEM images (a, c,e) and EDS spectra (b, d,f) of composite coatings, Agar disk-diffusion (a1, e1, e1) and spread plate (a2, c2, e2) results of coated specimens against *E. coli*bacterial for 24 h (a, b, a1, a2) HA−Zeo (c, d, c1, c22) 1ZnHA−Zeo (e, f, e1, e2) 2ZnHA−Zeo [219].

7. Surface treatment of IFI

The biocompatibility of implants with human tissues is crucial for successful fracture treatment. Implants made from materials such as stainless steel, titanium alloy, magnesium, Co-Cr alloy, polymers, and ceramics can interact with ions (e.g., Na+, K+, Cl-), proteins, and blood cells in body fluids. These interactions can lead to allergic reactions and reduce implant durability. For instance, metal ions released from stainless steel and Co-Cr alloys can cause local and systemic allergic responses in some patients, potentially leading to implant rejection or the need for revision surgery. Magnesium implants, which are biodegradable, interact with body fluids in a way that promotes gradual dissolution and natural bone regeneration. While this is beneficial for temporary implants, the rapid degradation of magnesium can sometimes lead to the release of hydrogen gas, which may cause complications if not properly managed. In addition to material interactions, bacterial infections are another significant concern in orthopedic implant surgery. Infections can occur during or after surgery, leading to implant failure and the need for additional surgical interventions. Bacteria can form biofilms on the surface of implants, making them resistant to antibiotics and the body's immune response. Preventing and managing infections is also crucial for the success of orthopedic implants [211]. To address these issues, surface treatments are often employed to enhance the corrosion resistance, wear resistance, antibacterial properties, and biocompatibility of implants.

For implants such as dental and artificial joints, wear resistance is particularly important. To improve the wear resistance of implants, it is common to apply a protective film on the implant surface. TiC or TiN protective layers can be formed on titanium alloy surfaces through various modification methods. A bio-inert TiC ceramic coating prepared on a Ti6Al4V substrate by laser cladding increased the wear resistance of the Ti6Al4V substrate by three times [212]. Additionally, new carbon nanocomposite coatings (CNC) can significantly improve the wear resistance of implants by approximately 250–650 times [213]. Corrosion resistance and wear resistance are equally important. The corrosion behavior of metal implants is significant, and the metal ions they release often have slight cytotoxicity. Currently, commonly used Ti-6Al-4V metal implants release Al and V ions, which can cause health problems [214,215]. Corrosion of Zn/Mg implants can lead to premature failure and fixation failure. Coating protection is an effective method to improve corrosion resistance. AT13 (Al_2O_3-13 wt% TiO_2)/HAP double-layer coated Ti-6Al-4V implants exhibit excellent corrosion resistance, polarization resistance, and microhardness compared to single-layer coated and uncoated implants [216]. The surface of WZ21 Mg alloy was modified by a silane coating impregnated with hexagonal boron nitride (HBN). In Hanks solution, the potential dynamic polarization and electrochemical impedance spectroscopy showed that the corrosion resistance of WZ21 Mg alloy with coated layer improved fivefold [217].

Some of the current commonly used implant materials lack bioactivity. Ceramics, titanium alloys, and stainless steel, as inert materials, cannot promote fracture healing. Therefore, surface modification technology can be used to impart bioactivity to implants. Bioactive coatings, such as hydroxyapatite (HA), polymer (PLA), and bioactive glasses (BG),

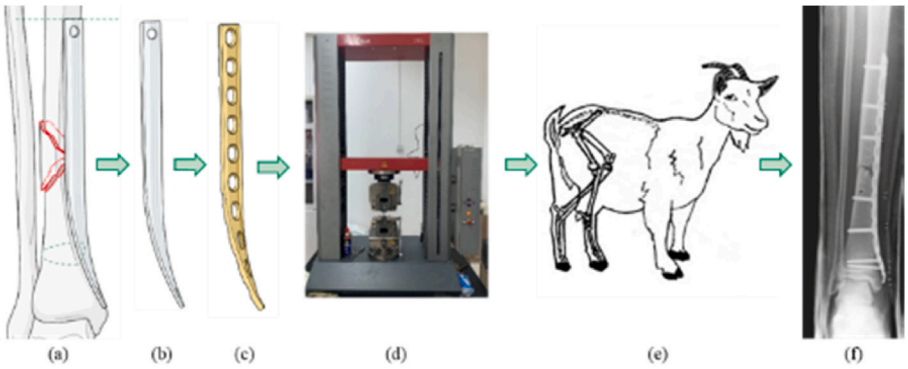

Fig. 22. The optimization design process of IFI: (a) The anatomical morphology of fractured bone, (b) The initial structure of IFI based on the anatomy of the bone, (c) Optimized design of IFI, (d) Mechanical test (e) Animal experiment, (f) Clinical follow-up.

are effective approaches. HA is commonly used because its composition is similar to the minerals in human bones, primarily composed of calcium phosphate, which matches the inorganic part of natural bone. This chemical similarity helps promote bone tissue attachment and integration [218]. Iqbal et al. [219] prepared Zn-doped HA with high corrosion resistance, providing sufficient Zn-plated corrosion protection for Mg surfaces and excellent antibacterial ability against *Escherichia coli*, as shown in Fig. 21, in which (a, b, a1, a2) is the results with HA−Zeo coating (c, d, c1, c22) is with 1ZnHA−Zeo coating (e, f, e1, e2) is 2ZnHA−Zeo. Jiang et al. [220]prepared an HA coating on titanium alloy by hydrothermal method, as shown in Fig. 21(g) and (h), For sample No. 1, No. 2, and No. 3, are drug loaded and HA coated titanium alloy bone nail, non-coated titanium alloy bone nail and HA coated titanium alloy bone nail, respectively. Both cell adhesion and animal experiments showed that HA coating has good biocompatibility and promotes new bone formation. Currently, the co-precipitation method is often used to dope metal ions such as Zn^{2+}, Mg^{2+}, and Cu^{2+} into HA to prepare multifunctional coatings. Shanmugam et al. [221]studied the preparation of copper-substituted HA and fluoroapatite ($Ca_5F(PO_4)^3$) coatings by co-precipitation method and detected good antibacterial activity. Additionally, microstructures can be etched on the surface by laser or prepared by chemical methods to promote cell attachment. Ni et al. [222]used plasma electrolytic oxidation (PEO) technology to prepare porous Mg-TiO_2 coating on titanium surfaces, showing good biocompatibility and better cell adhesion. Ma et al. [223]prepared a porous titanium alloy scaffold customized for bone defects through 3D printing. The 3D printed porous structure promoted the formation of vascularized bone tissue, and the new bone formed a stable bond with the implant. To avoid postoperative infection caused by implants, antibacterial technologies such as surface modification and antibacterial materials have been applied in clinical medicine. Surface modification can effectively prevent biofilm formation on implant materials by causing cell damage to attached bacteria, inhibiting bacterial adhesion, and releasing antibacterial agents to inhibit bacterial reproduction. Antibacterial materials, as passive coatings, can kill bacteria on contact. Various antibacterial agents with bactericidal effects are commonly used to prepare antibacterial coatings on orthopedic implants. Generally used metal antibacterial materials include Zn [224], Ag [225], Cu [226]. To prevent cell adhesion, surface grafting, and layer-by-layer self-assembly to fix hydrophilic macromolecules on the material surface to construct a hydrophilic layer has become a possible method to resist bacterial adhesion. Hydrophilic polymers such as polyethylene glycol (PEG), zwitterionic polymers, hyaluronic acid (HA), and sodium alginate have strong activity and are non-toxic [227]. Additionally, photosensitizers like TiO2 and ICG generate reactive oxygen species (ROS) when exposed to light, which can destroy polysaccharides, the main components of biofilm surfaces, thus having a bactericidal effect on drug-resistant bacteria [228]. Ideal implants should have both antibacterial and osteogenic properties, making multifunctional composite coatings a hot topic in current research. Chen et al. [212]prepared calcium phosphate (CaP) intermediate layers and PLA composite layers with different sealing degrees on Zn-Mn-Mg alloys by hydrothermal (HT) and dip coating methods. The Zn release rate was effectively controlled, and the composite coating significantly improved cell compatibility.

(g) is the CT image of the rabbit femur after 2 months of implantation, (h) is the percentages of new bone volume. No.1 is the drug loaded and HA coated titanium alloy bone nail CT, No.2 is the non-coated titanium alloy bone nail CT, No.3 is the HA coated titanium alloy bone nail CT [220].

Over the past few decades, there has been a significant global surge in the demand for orthopedic implants. Long-term and stable fixation of implants can reduce pain and the risk of secondary surgery for patients. Surface treatment can give implants multiple functions, but the detection of multifunctionality is still in the cell experiment stage, and a large number of animal experiments are still needed to ensure the safety and reliability of implants.

8. Challenges and prospects

With the development of material science, medicine, and computational science, remarkable progress has been made in design methods medical biomaterials, fracture healing theory, fracture healing simulation model, and experimental methods, but there are still some problems that need to be further studied. Firstly, the biomaterial used for IFI is still mainly inert metal. The functional biomaterials have not been fully applied to the practice due to high manufacturing cost, difficult processing and unclear biological characteristics. Secondly, mechanical responses are often used as evaluation indexes in the existing IFI design. A comprehensive evaluation method based on fracture healing theory has not been established. In addition, there are few researches on collaborative designs with multiple design factors in IFI design. And the research on the optimization design methods of IFI with functional characteristics, such stiffness gradient and time-changeable stiffness, is less.

The general process of optimization design of IFI is shown in Fig. 22 (a)–(f). (1) The initial structure of IFI based on the anatomical morphology of fractured bone is established and the appropriate material is selected according to the load conditions of fracture bone. (2) The reasonable design factors according to the specific design objects are selected and the IFI is optimized based on the optimization mathematical model considering fracture healing theory. (3) The mechanical experiment is conducted to verify the safety of the optimization design result. (4) The animal experiment is carried out to evaluate the biocompatibility of IFI. (5) The clinical follow-up is conducted to observe the clinical therapeutic effect of IFI.

According to the design requirements proposed in Section 2, the changing trend of structural stiffness of the ideal IFI with time course in fracture healing process is shown in Fig. 21. In the period of bone

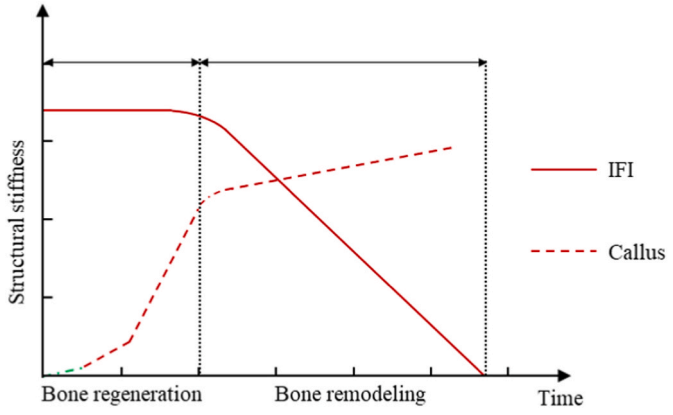

Fig. 23. The changing trend of structure stiffness of ideal IFI and callus during fracture healing.

regeneration, the structural stiffness is basically unchanged, which can ensure the stable biomechanical environment to be established. During the period of bone remodeling, the structural stiffness decreases gradually, so the bone gradually bears more load. Therefore, the ideal IFI should have different time-changing stiffness characteristics at different healing process. Implant made of only one type of material can hardly fulfil multiple demands of fracture fixations. Composite implants made of multi biodegradable material or single biodegradable material structure with coating attract attention from both surgeons and material scientists. The IFI with multi material composite structure is composed of two materials with different material properties and degradation rates. The biodegradable IFI with coating consists of biodegradable base structure and coating. Thus, the structural stiffness of IFI decreases slowly in the early stage of degradation process and relatively quickly in the late stage of degradation process. Additionally, hybrid fixation system, such as Mg and Ti hybrid fixation implants, is also a promising solution.

Based on the design process and ideal mechanical properties of the IFI, some future research contents are summarized as follows,

(1) In order to understand the effect of IFI degradation on fracture healing,the coupled model of IFI degradation-mechanics analysis and fracture healing simulation should be established. On the basis of this model, the interaction mechanism between structure degradation and the change of mechanical properties can be analyzed by the simulation of the structural degradation, and the relationship between fracture healing and the time-changeable stiffness of IFI can be understood.
(2) For the optimization design of biodegradable IFI, the topology optimization method of biodegradable structure considering time-changing stiffness should be studied. First, the sensitivity of the degradation process to the structural mechanical properties and fracture healing effect needs to be deduced. Then, the structure of IFI with required time-changeable stiffness characteristics can be obtained by designing the distribution of multi biodegradable materials with different material properties and degradation rates in design domain using topology optimization method.
(3) The coating can delay the degradation of base structure, and the degradable structure with coating can be applied to the design of ideal IFI. Therefore, the optimization design method of biodegradable IFI with coating should be studied. First, the designability of coating needs to be analyzed. Then, the ideal IFI can be obtained by the simultaneous design of base structure and coating.
(4) To achieve full lifecycle design, the comprehensive study on design, manufacture and experimental of biodegradable IFI should be studied. For one thing, the integration of design and manufacturing can be realized by setting additive manufacturing constraints in IFI design process. For another, the experimental method for evaluating the time-changing stiffness characteristics of biodegradable IFI needs to be further studied (see Fig. 23).

Compliance with ethics guidelines

The authors declare that they have no conflict of interest.

This study does not contain any studies with human or animal subjects performed by any of the authors.

Acknowledgments

The work was supported by the Natural Science Foundation of Shanghai (22ZR1442800), and National Natural Science Foundation of China (Grant No. 51975380, 52375257).

References

[1] Tejwani N, Polonet D, Wolinsky PR. External fixation of tibial fractures. JAAOS - Journal of the American Academy of Orthopaedic Surgeons 2015;(2):23.
[2] Perren SM. Evolution of the internal fixation of long bone fractures - the scientific basis of biological internal fixation: choosing a new balance between stability and biology. J Bone Joint Surg 2002:1093–110. 84B(8).
[3] Buckley RE, Moran CG, Apivatthakakul T. *AO Principles of fracture management*, in *AO Principles of fracture management*. Stuttgart: Georg Thieme Verlag KG; 2018.
[4] Perren SM. Evolution and rationale of locked internal fixator technology. Introductory remarks. Injury 2001:32. Suppl 2: p. B3-9.
[5] Stiffler KS. Internal fracture fixation. Clin Tech Small Anim Pract 2004;19(3): 105–13.
[6] Marsell R, Einhorn TA. The biology of fracture healing. Injury-international Journal of The Care of The Injured 2011;42(6):551–5.
[7] Claes L, Recknagel S, Ignatius A. Fracture healing under healthy and inflammatory conditions. Nat Rev Rheumatol 2012;8(3):133–43.
[8] Perren SM, Klaue K, Pohler O, Predieri M, Steinemann S, Gautier E. The limited contact dynamic compression plate (LC-DCP). Arch Orthop Trauma Surg 1990; 109(6):304–10.
[9] European journal of orthopaedic surgery & traumatology. In: Kehr P, Richard E, Christopher G, Moran, Theerachai Apivatthakakul, editors. AO principles of fracture management 2 vols.. 3rd ed. 2018. 28(7): pp. 1453–1453.
[10] Isaksson H, Wilson W, van Donkelaar CC, Huiskes R, Ito K. Comparison of biophysical stimuli for mechano-regulation of tissue differentiation during fracture healing. J Biomech 2006;39(8):1507–16.
[11] Al-Tamimi AA, Al-Qahtani MS, Liu F, Alkahtani A, Peach C, Bártolo PJ. A review on powder bed fusion additive manufacturing for metallic fixation implants. In: Bidanda B, Bártolo PJ, editors. Virtual prototyping & bio manufacturing in medical applications; 2021. p. 235–56. Springer International Publishing: Cham.
[12] Mehboob H, Kim J, Mehboob A, Chang S-H. How post-operative rehabilitation exercises influence the healing process of radial bone shaft fractures fixed by a composite bone plate. Compos Struct 2017;159:307–15.
[13] Jagodzinski M, Krettek C. Effect of mechanical stability on fracture healing - an update. Injury-International Journal of the Care of the Injured 2007;38:S3–10.
[14] Sigurdsen U, Reikeras O, Utvag SE. The influence of compression on the healing of experimental tibial fractures. Injury-International Journal of the Care of the Injured 2011;42(10):1152–6.
[15] Wolff J. The classic: on the inner architecture of bones and its importance for bone growth. Clin Orthop Relat Res 2010;468(4):1056–65.
[16] Wolff J. The classic: on the theory of fracture healing. Clin Orthop Relat Res 2010; 468(4):1052–5.
[17] Perren SM. The concept of biological plating using the limited contact dynamic compression plate(LC-DCP). Injury-international Journal of The Care of The Injured 1991;22(1):1–41.
[18] Hori RY, Lewis JL. Mechanical properties of the fibrous tissue found at the bone-cement interface following total joint replacement. J Biomed Mater Res 1982;16 (6):911–27.
[19] Lacroix D, Prendergast PJ. A mechano-regulation model for tissue differentiation during fracture healing: analysis of gap size and loading. J Biomech 2002;35(9): 1163–71.
[20] Claes LE, Heigele CA. Magnitudes of local stress and strain along bony surfaces predict the course and type of fracture healing. J Biomech 1999;32(3):255–66.
[21] Mehboob H, Son D-S, Chang S-H. Finite element analysis of tissue differentiation process of a tibia with various fracture configurations when a composite intramedullary rod was applied. Compos Sci Technol 2013;80:55–65.
[22] Armstrong CG, Mow VC. Variations in the intrinsic mechanical properties of human articular cartilage with age, degeneration, and water content. JBJS 1982; (1):64.
[23] Ochoa J. Permeability of bovine cancellous bone. Trans. 38th ORS 1992:162.
[24] Johnson MW, Chakkalakal DA, Harper RA, Katz JL, Rouhana SW. Fluid flow in bone in vitro. J Biomech 1982;15(11):881–5.

[25] Jurvelin JS, Buschmann MD, Hunziker EB. Optical and mechanical determination of Poisson's ratio of adult bovine humeral articular cartilage. J Biomech 1997;30(3):235–41.
[26] Cowin SC. *Bone poroelasticity.* journal of biomechanics 1999;32(3):217–38.
[27] Baumeister T, Marks LS. Standard handbook for mechanical engineers. 1967.
[28] Tepic S, Macirowski T, Mann RW. Mechanical properties of articular cartilage elucidated by osmotic loading and ultrasound. Proceedings of the National Academy of Sciences 1983;80(11):3331–3.
[29] Smit TH, Huyghe JM, Cowin SC. Estimation of the poroelastic parameters of cortical bone. J Biomech 2002;35(6):829–35.
[30] Mow VC, Kuei SC, Lai WM, Armstrong CG. Biphasic creep and stress relaxation of articular cartilage in compression: theory and experiments. J Biomech Eng 1980;102(1):73–84.
[31] Schaffler MB, Burr DB. Stiffness of compact bone: effects of porosity and density. J Biomech 1988;21(1):13–6.
[32] Taylor M, Prendergast PJ. Four decades of finite element analysis of orthopaedic devices: where are we now and what are the opportunities? J Biomech 2015;48(5):767–78.
[33] Uzer G, Yildiz F, Batar S, Bozdag E, Kuduz H, Bilsel K. Biomechanical comparison of three different plate configurations for comminuted clavicle midshaft fracture fixation. J Shoulder Elbow Surg 2017;26(12):2200–5.
[34] Bigham-Sadegh A, Oryan A. Selection of animal models for pre-clinical strategies in evaluating the fracture healing, bone graft substitutes and bone tissue regeneration and engineering. Connect Tissue Res 2015;56(3):175–94.
[35] Qiao B, Zhou D, Dai Z, Zhao W, Yang Q, Xu Y, et al. Bone Plate composed of a ternary nanohydroxyapatite/polyamide 66/glass fiber composite: biocompatibility in vivo and internal fixation for canine femur fractures. Adv Funct Mater 2019;29(22):1808738.
[36] Borens O, Kloen P, Richmond J, Roederer G, Levine DS, Helfet DL. Minimally invasive treatment of pilon fractures with a low profile plate: preliminary results in 17 cases. Arch Orthop Trauma Surg 2009;129(5):649–59.
[37] Yoda N, Zheng K, Chen J, Liao Z, Koyama S, Peck C, et al. Biomechanical analysis of bone remodeling following mandibular reconstruction using fibula free flap. Med Eng Phys 2018;56:1–8.
[38] Lee J-H, Park K-C, Lim S-J, Kwon K-B, Kim JW. Surgical outcomes of simple distal femur fractures in elderly patients treated with the minimally invasive plate osteosynthesis technique: can percutaneous cerclage wiring reduce the fracture healing time? Arch Orthop Trauma Surg 2020.
[39] Stoffel K, Dieter U, Stachowiak G, Gachter A, Kuster MS. Biomechanical testing of the LCP - how can stability in locked internal fixators be controlled? Injury-International Journal of the Care of the Injured 2003;34:11–9.
[40] Devika D, Arumaikkannu G. Evaluation of mechanical behaviour of bone, implant and bone-implant interface by numerical simulation of two surgical fixation procedures using Finite Element Analysis. IJCAT 2011;42:225–32.
[41] Gutwald R, Jaeger R, Lambers FM. Customized mandibular reconstruction plates improve mechanical performance in a mandibular reconstruction model. Comput Methods Biomech Biomed Eng 2017;20(4):426–35.
[42] Yu B, Chen W-C, Lee P-Y, Lin K-P, Lin K-J, Tsai C-L, et al. Biomechanical comparison of conventional and anatomical calcaneal plates for the treatment of intraarticular calcaneal fractures - a finite element study. Comput Methods Biomech Biomed Eng 2016;19(13):1363–70.
[43] Wang R, Liu Y, Wang JH, Baur DA. Effect of interfragmentary gap on the mechanical behavior of mandibular angle fracture with three fixation designs: a finite element analysis. J Plast Reconstr Aesthetic Surg 2017;70(3):360–9.
[44] Nurettin D, Burak B. Feasibility of carbon-fiber-reinforced polymer fixation plates for treatment of atrophic mandibular fracture: a finite element method. J Cranio-Maxillofacial Surg 2018;46(12):2182–9.
[45] Ganesh VK, Ramakrishna K, Ghista DN. Biomechanics of bone-fracture fixation by stiffness-graded plates in comparison with stainless-steel plates. Biomed Eng Online 2005;4(1):46.
[46] Ramakrishna K, Sridhar I, Sivashanker S, Ganesh VK, Ghista DN. *Analysis of an internal fixation of A long bone fracture.* Journal of mechanics in medicine and biology 2005;5(1):89–103.
[47] Fan Y, Xiu K, Duan H, Zhang M. Biomechanical and histological evaluation of the application of biodegradable poly-l-lactic cushion to the plate internal fixation for bone fracture healing. Clin BioMech 2008;23:S7–16.
[48] Benli S, Aksoy S, Havıtcıoğlu H, Kucuk M. Evaluation of bone plate with low-stiffness material in terms of stress distribution. J Biomech 2008;41(15):3229–35.
[49] Barua E, Das S, Deoghare AB. Development of computational Tibia model to investigate stress shielding effect at healing stages. Mater Today Proc 2018;5(5):13267–75.
[50] Duda GN, Mandruzzato F, Heller M, Kassi JP, Khodadadyan C, Haas NP. Mechanical conditions in the internal stabilization of proximal tibial defects. Clin BioMech 2002;17(1):64–72.
[51] Lee C-H, Shih K-S, Hsu C-C, Cho T. Simulation-based particle swarm optimization and mechanical validation of screw position and number for the fixation stability of a femoral locking compression plate. Med Eng Phys 2014;36(1):57–64.
[52] Samiezadeh S, Tavakkoli Avval P, Fawaz Z, Bougherara H. On optimization of a composite bone plate using the selective stress shielding approach. Journal of the Mechanical Behavior of Biomedical Materials 2015;42:138–53.
[53] Izaham R, Kadir MRA, Rashid AHA, Hossain MG, Kamarul T. Finite element analysis of Puddu and Tomofix plate fixation for open wedge high tibial osteotomy. Injury-International Journal of the Care of the Injured 2012;43(6):898–902.
[54] Pauwels F. A new theory on the influence of mechanical stimuli on the differentiation of supporting tissue. The tenth contribution to the functional anatomy and causal morphology of the supporting structure. Zeitschrift fur Anatomie und Entwicklungsgeschichte 1960;121:478–515.
[55] Carter DR, Blenman PR, Beaupré GS. Correlations between mechanical stress history and tissue differentiation in initial fracture healing. J Orthop Res 1988;6(5):736–48.
[56] Carter DR, Beaupré GS, Giori NJ, Helms JA. Mechanobiology of skeletal regeneration. Clin Orthop Relat Res 1998;(355 Suppl):S41–55.
[57] Perren Sm CJ. The concept of interfragmentary strain. Current Concepts of Internal Fixation of Fractures 1980:63–77.
[58] Claes L, Augat P, Suger G, Wilke HJ. Influence of size and stability of the osteotomy gap on the success of fracture healing. Journal of orthopaedic research. official publication of the Orthopaedic Research Society 1997;15(4):577–84.
[59] Claes L, Heigele CA, Neidlingerwilke C, Kaspar D, Seidl W, Margevicius K, et al. Effects of mechanical factors on the fracture healing process. Clinical orthopaedics and related research 1998;355(355):132–47.
[60] Huiskes R, VanDriel WD, Prendergast PJ, Soballe K. A biomechanical regulatory model for periprosthetic fibrous-tissue differentiation. J Mater Sci Mater Med 1997;8(12):785–8.
[61] Prendergast PJ. Finite element models in tissue mechanics and orthopaedic implant design. Clin BioMech 1997;12(6):343–66.
[62] Prendergast PJ, Huiskes R, Søballe K. Biophysical stimuli on cells during tissue differentiation at implant interfaces. J Biomech 1997;30(6):539–48.
[63] Lacroix D, Prendergast PJ, Li G, Marsh D. Biomechanical model to simulate tissue differentiation and bone regeneration: application to fracture healing. Med Biol Eng Comput 2002;40(1):14–21.
[64] Perez MA, Prendergast PJ. Random-walk models of cell dispersal included in mechanobiological simulations of tissue differentiation. J Biomech 2007;40(10):2244–53.
[65] Isaksson H, van Donkelaar CC, Huiskes R, Ito K. Corroboration of mechanoregulatory algorithms for tissue differentiation during fracture healing: comparison with in vivo results. J Orthop Res 2006;24(5):898–907.
[66] Isaksson H, van Donkelaar CC, Huiskes R, Ito K. A mechano-regulatory bone-healing model incorporating cell-phenotype specific activity. J Theor Biol 2008;252(2):230–46.
[67] Kelly DJ, Prendergast PJ. Mechano-regulation of stem cell differentiation and tissue regeneration in osteochondral defects. J Biomech 2005;38(7):1413–22.
[68] Gomez-Benito MJ, Garcia-Aznar JM, Kuiper JH, Doblare M. Influence of fracture gap size on the pattern of long bone healing: a computational study. J Theor Biol 2005;235(1):105–19.
[69] Gómez-Benito MJ, García-Aznar JM, Kuiper JH, Doblaré M. A 3D computational Simulation of fracture callus formation: Influence of the Stiffness of the external fixator. J Biomech Eng 2006;128(3):290–9.
[70] Kang K-T, Park J-H, Kim H-J, Lee H-M, Lee K-I, Jung H-H, et al. Study on differentiation of mesenchymal stem cells by mechanical stimuli and an algorithm for bone fracture healing. Tissue Engineering and Regenerative Medicine 2011;8(4):359–70.
[71] Isaksson H, Comas O, van Donkelaar CC, Mediavilla J, Wilson W, Huiskes R, et al. Bone regeneration during distraction osteogenesis: mechano-regulation by shear strain and fluid velocity. J Biomech 2007;40(9):2002–11.
[72] Garcia-Aznar JM, Kuiper JH, Gomez-Benito MJ, Doblare M, Richardson JB. Computational simulation of fracture healing: influence of interfragmentary movement on the callus growth. J Biomech 2007;40(7):1467–76.
[73] Reina-Romo E, Gomez-Benito MJ, Garcia-Aznar JM, Dominguez J, Doblare M. Growth mixture model of distraction osteogenesis: effect of pre-traction stresses. Biomechanics and Modeling in Mechanobiology 2010;9(1):103–15.
[74] Reina-Romo E, Gomez-Benito MJ, Garcia-Aznar JM, Dominguez J, Doblare M. Modeling distraction osteogenesis: analysis of the distraction rate. Biomechanics and Modeling in Mechanobiology 2009;8(4):323–35.
[75] Ament C, Hofer EP. *A fuzzy logic model of fracture healing.* Journal of Biomechanics 2000;33(8):961–8.
[76] Shefelbine SJ, Augat P, Claes L, Simon U. Trabecular bone fracture healing simulation with finite element analysis and fuzzy logic. J Biomech 2005;38(12):2440–50.
[77] Chen G, Niemeyer F, Wehner T, Simon U, Schuetz MA, Pearcy MJ, et al. Simulation of the nutrient supply in fracture healing. J Biomech 2009;42(15):2575–83.
[78] Simon U, Augat P, Utz M, Claes L. *A numerical model of the fracture healing process that describes tissue development and revascularisation.* Computer Methods in Biomechanics and Biomedical Engineering 2011;14(1):79–93.
[79] Checa S, Prendergast PJ. *A mechanobiological Model for tissue Differentiation that includes angiogenesis: a lattice-based modeling approach.* Annals of biomedical engineering 2009;37(1):129–45.
[80] Frost HM. A determinant of bone architecture. The minimum effective strain. Clinical orthopaedics and related research 1983;175:286–92.
[81] Frost HM. Vital biomechanics: Proposed general concepts for skeletal adaptations to mechanical usage. Calcif Tissue Int 1988;42(3):145–56.
[82] Frost HM. Bone's mechanostat: a 2003 update. Anat Rec Part A: Discoveries in Molecular, Cellular, and Evolutionary Biology 2003;275A(2):1081–101.
[83] Weinans H, Huiskes R, Grootenboer HJ. The behavior of adaptive bone-remodeling simulation models. J Biomech 1992;25(12):1425–41.
[84] Bourauel C, Vollmer D, Jäger A. Application of bone remodeling theories in the simulation of orthodontic tooth movements. J Orofac Orthop/Fortschritte Kieferorthop 2000;61(4):266–79.
[85] Mellal A, Wiskott HWA, Botsis J, Scherrer SS, Belser UC. Stimulating effect of implant loading on surrounding bone - comparison of three numerical models and validation by in vivo data. Clin Oral Implants Res 2004;15(2):239–48.

[86] Li I, Li H, Shi L, Fok ASL, Ucer C, Deulin H, et al. A mathematical model for simulating the bone remodeling process under mechanical stimulus. Dent Mater 2007;23(9):1073–8.
[87] Rungsiyakull C, Chen J, Rungsiyakull P, Li W, Swain M, Li Q. Bone's responses to different designs of implant-supported fixed partial dentures. Biomechanics and Modeling in Mechanobiology 2015;14(2):403–11.
[88] Nikolova MP, Chavali MS. Recent advances in biomaterials for 3D scaffolds: a review. Bioact Mater 2019;4:271–92.
[89] Mehboob H, Chang S-H. Application of composites to orthopedic prostheses for effective bone healing: a review. Compos Struct 2014;118:328–41.
[90] Chen Q, Thouas GA. *Metallic implant biomaterials.* Materials science & engineering R-reports 2015;87:1–57.
[91] Zheng YF, Gu XN, Witte F. Biodegradable metals. Mater Sci Eng R Rep 2014;77:1–34.
[92] Safranski D, Dupont K, Gall K. Pseudoelastic NiTiNOL in orthopaedic applications. Shape Memory and Superelasticity 2020.
[93] Han Q, Wang C, Chen H, Zhao X, Wang J. Porous tantalum and titanium in orthopedics: a review. Acs biomaterials science & engineering 2019;5(11):5798–824.
[94] Dorozhkin SV. Bioceramics of calcium orthophosphates. Biomaterials 2010;31(7):1465–85.
[95] Dorozhkin SV. Current state of bioceramics. Journal of ceramic science and technology 2018;9(4):353–70.
[96] Bradley JS, Hastings GW, Johnson-Nurse C. Carbon fibre reinforced epoxy as a high strength, low modulus material for internal fixation plates. Biomaterials 1980;1(1):38–40.
[97] Peluso G, Ambrosio L, Cinquegrani M, Nicolais L, Saiello S, Tajana G. Rat peritoneal immune response to carbon fibre reinforced epoxy composite implants. Biomaterials 1991;12(2):231–5.
[98] P. Aihemaiti, R. Jia, W. Aiyiti, H. Jiang and A. Kasimu, *Study on 3D printing process of continuous polyglycolic acid fiber-reinforced polylactic acid degradable composites*. IJBD (Int J Behav Dev) 9(4).
[99] Mehboob H, Bae J-H, Han M-G, Chang S-H. Effect of air plasma treatment on mechanical properties of bioactive composites for medical application: composite preparation and characterization. Compos Struct 2016;143:23–32.
[100] Mehboob H, Mehboob A, Abbassi F, Ahmad F, Chang S-H. Finite element analysis of biodegradable Ti/polyglycolic acid composite bone plates based on 3D printing concept. Compos Struct 2022;289:115521.
[101] Uhthoff HK, Poitras P, Backman DS. Internal plate fixation of fractures: short history and recent developments. J Orthop Sci 2006;11(2):118–26.
[102] Bostman O, Viljanen J, Salminen S, Pihlajamaki H. Response of articular cartilage and subchondral bone to internal fixation devices made of poly-L-lactide: a histomorphometric and microradiographic study on rabbits. Biomaterials 2000;21(24):2553–60.
[103] Nagels J, Stokdijk M, Rozing PM. Stress shielding and bone resorption in shoulder arthroplasty. Journal of Shoulder and Elbow Surgery 2003;12(1):35–9.
[104] Jacobs JJ, Gilbert JL, Urban RM. Current concepts review - corrosion of metal orthopaedic implants. Journal of bone and joint surgery. American Volume 1998;80(2):268–82.
[105] Jacobs JJ, Hallab NJ, Skipor AK, Urban RM. Metal degradation products: a cause for concern in metal-metal bearings? Clin Orthop Relat Res 2003;417:139–47.
[106] Lhotka C, Szekeres T, Steffan I, Zhuber K, Zweymüller K. Four-year study of cobalt and chromium blood levels in patients managed with two different metal-on-metal total hip replacements. Journal of Orthopaedic Research 2003;21(2):189–95.
[107] Reith G, Schmitz-Greven V, Hensel KO, Schneider MM, Tinschmann T, Bouillon B, et al. Metal implant removal: benefits and drawbacks - a patient survey. BMC Surg 2015;15:8.
[108] Stradiotti P, Curti A, Castellazzi G, Zerbi A. Metal-related artifacts in instrumented spine. Techniques for reducing artifacts in CT and MRI: state of the art. European Spine Journal 2009;18:S102–8.
[109] Tian L, Tang N, Ngai T, Wu C, Ruan Y, Huang L, et al. Hybrid fracture fixation systems developed for orthopaedic applications: a general review. Journal of Orthopaedic Translation 2019;16:1–13.
[110] Shan Z, Xie X, Wu X, Zhuang S, Zhang C. Development of degradable magnesium-based metal implants and their function in promoting bone metabolism (A review). Journal of Orthopaedic Translation 2022;36:184–93.
[111] Yang Y, He C, E D, Yang W, Qi F, Xie D, et al. Mg bone implant: features, developments and perspectives. Mater Des 2020:185.
[112] Wang JL, Xu JK, Hopkins C, Chow DH, Qin L. Biodegradable magnesium-based Implants in orthopedics-A general Review and perspectives. Adv Sci 2020;7(8):1902443.
[113] Gu X, Zheng Y, Cheng Y, Zhong S, Xi T. In vitro corrosion and biocompatibility of binary magnesium alloys. Biomaterials 2009;30(4):484–98.
[114] Francis A, Yang Y, Virtanen S, Boccaccini AR. Iron and iron-based alloys for temporary cardiovascular applications. J Mater Sci Mater Med 2015;26(3):138.
[115] Peuster M, Hesse C, Schloo T, Fink C, Beerbaum P, von Schnakenburg C. Long-term biocompatibility of a corrodible peripheral iron stent in the porcine descending aorta. Biomaterials 2006;27(28):4955–62.
[116] Pierson D, Edick J, Tauscher A, Pokorney E, Bowen P, Gelbaugh J, et al. A simplified in vivo approach for evaluating the bioabsorbable behavior of candidate stent materials. J Biomed Mater Res B Appl Biomater 2012;100B(1):58–67.
[117] Moravej M, Mantovani D. Biodegradable metals for cardiovascular stent application: interests and new opportunities. Int J Mol Sci 2011;12(7):4250–70.
[118] Hernandez-Escobar D, Champagne S, Yilmazer H, Dikici B, Boehlert CJ, Hermawan H. Current status and perspectives of zinc-based absorbable alloys for biomedical applications. Acta Biomater 2019;97:1–22.
[119] Su Y, Cockerill I, Wang Y, Qin Y-X, Chang L, Zheng Y, et al. Zinc-based Biomaterials for Regeneration and therapy. Trends Biotechnol 2019;37(4):428–41.
[120] Petrini L, Migliavacca F. Biomedical applications of shape memory alloys. Journal of Metallurgy 2011:501483 (15 pp.)-501483 (15 pp.).
[121] Chen W, Dai N, Wang JQ, Liu H, Li DW, Liu LL. Personalized design of functional gradient bone tissue engineering scaffold. Journal of Biomechanical Engineering-Transactions of the Asme 2019;11:141.
[122] Ghouse S, Reznikov N, Boughton OR, Babu S, Ng KCG, Blunn G, et al. The design and in vivo testing of a locally stiffness-matched porous scaffold. Appl Mater Today 2019;15:377–88.
[123] Zhang X-Y, Fang G, Leeflang S, Zadpoor AA, Zhou J. Topological design, permeability and mechanical behavior of additively manufactured functionally graded porous metallic biomaterials. Acta Biomater 2019;84:437–52.
[124] Qin Y, Wen P, Guo H, Xia D, Zheng Y, Jauer L, et al. Additive manufacturing of biodegradable metals: current research status and future perspectives. Acta Biomater 2019;98:3–22.
[125] Wang J-C, Dommati H, Hsieh S-J. Review of additive manufacturing methods for high-performance ceramic materials. Int J Adv Manuf Technol 2019;103(5–8):2627–47.
[126] Ali W, Mehboob A, Han M-G, Chang S-H. Effect of fluoride coating on degradation behaviour of unidirectional Mg/PLA biodegradable composite for load-bearing bone implant application. Compos Appl Sci Manuf 2019:124.
[127] Ali W, Mehboob A, Han M-G, Chang S-H. Experimental study on degradation of mechanical properties of biodegradable magnesium alloy (AZ31) wires/poly (lactic acid) composite for bone fracture healing applications. Compos Struct 2019;210:914–21.
[128] Mehboob A, Mehboob H, Chang S-H. Evaluation of unidirectional BGF/PLA and Mg/PLA biodegradable composites bone plates-scaffolds assembly for critical segmental fractures healing. Compos Appl Sci Manuf 2020;135:105929.
[129] Mehboob A, Rizvi SHA, Chang S-H, Mehboob H. Comparative study of healing fractured tibia assembled with various composite bone plates. Compos Sci Technol 2020:108248.
[130] Zagho MM, Hussein EA, Elzatahry AA. Recent overviews in functional polymer composites for biomedical applications. Polymers 2018;(7):10.
[131] Bottlang M, Tsai S, Bliven EK, von Rechenberg B, Kindt P, Augat P, et al. Dynamic stabilization of simple fractures with active plates delivers stronger healing than conventional compression plating. J Orthop Trauma 2017;31(2):71–7.
[132] Janssen KW, Biert J, Van Kampen A. Treatment of distal tibial fractures: plate versus nail: a retrospective outcome analysis of matched pairs of patients. Int Orthop 2007;31(5):709–14.
[133] Rosa N, Marta M, Vaz M, Tavares SMO, Simoes R, Magalhaes FD, et al. Intramedullary nailing biomechanics: evolution and challenges. Proc IME H J Eng Med 2019;233(3):295–308.
[134] Gupta A, Maharjan A, Kim BS. Shape memory polyurethane and its composites for various applications. Applied Sciences-Basel 2019;9(21):29.
[135] Zhang Y, Zhao X, Tang Y, Zhang C, Xu S, Xie Y. Application of Ni-Ti Alloy connector for the treatment of comminuted coronal plane supracondylar-condylar femoral fractures: a retrospective review of 21 patients. BMC Muscoskel Disord 2013;14(1):355.
[136] Murakami K, Yamamoto K, Sugiura T, Kawakami M, Horita S, Kirita T. Biomechanical analysis of poly-L-lactic acid and titanium plates fixated for mandibular symphyseal fracture with a conservatively treated unilateral condylar fracture using the three-dimensional finite element method. Dent Traumatol 2015;31(5):396–402.
[137] Mehboob H, Chang S-H. Effect of structural stiffness of composite bone plate–scaffold assembly on tibial fracture with large fracture gap. Compos Struct 2015;124:327–36.
[138] Kim H-J, Kim S-H, Chang S-H. Finite element analysis using interfragmentary strain theory for the fracture healing process to which composite bone plates are applied. Compos Struct 2011;93(11):2953–62.
[139] Kim SH, Chang SH, Son DS. Finite element analysis of the effect of bending stiffness and contact condition of composite bone plates with simple rectangular cross-section on the bio-mechanical behaviour of fractured long bones. Compos B Eng 2011;42(6):1731–8.
[140] Zaheer MU, Mehboob H, Mehboob A, Chang SH. Evaluation of the effect of bone plate modulus on the early bone healing of fractured tibia. Compos B Eng 2022:233.
[141] Son DS, Chang SH. The simulation of bone healing process of fractured tibia applied with composite bone plates according to the diaphyseal oblique angle and plate modulus. Compos B Eng 2013;45(1):1325–35.
[142] Lima DD, Mantri SA, Mikler CV, Contieri R, Yannetta CJ, Campo KN, et al. Laser additive processing of a functionally graded internal fracture fixation plate. Mater Des 2017;130:8–15.
[143] Mehboob H, Chang S-H. Evaluation of the development of tissue phenotypes: bone fracture healing using functionally graded material composite bone plates. Compos Struct 2014;117:105–13.
[144] Mehboob H, Chang S-H. Evaluation of healing performance of biodegradable composite bone plates for a simulated fractured tibia model by finite element analysis. Compos Struct 2014;111:193–204.
[145] Vijayavenkataraman S, Gopinath A, Lu WF. A new design of 3D-printed orthopedic bone plates with auxetic structures to mitigate stress shielding and

improve intra-operative bending. Bio-Design and Manufacturing 2020;3(2):98–108.
[146] Mehboob H, Chang S-H. Optimal design of a functionally graded biodegradable composite bone plate by using the Taguchi method and finite element analysis. Compos Struct 2015;119:166–73.
[147] Synek A, Baumbach SF, Pahr DH. Towards optimization of volar plate fixations of distal radius fractures: using finite element analyses to reduce the number of screws. Clin BioMech 2021;82:105272.
[148] Subasi O, Oral A, Lazoglu I. A novel adjustable locking plate (ALP) for segmental bone fracture treatment. Injury-International Journal of the Care of the Injured 2019;50(10):1612–9.
[149] Jabran A, Peach C, Zou Z, Ren L. Parametric design optimisation of proximal humerus plates based on finite element method. Ann Biomed Eng 2019;47(2):601–14.
[150] Korkmaz HH. Evaluation of different miniplates in fixation of fractured human mandible with the finite element method. Oral Surg Oral Med Oral Pathol Oral Radiol Endod 2007;6:103. E1-E13.
[151] de Oliveira KP, de Moraes PH, da Silva JSP, de Queiroz WF, Germano AR. In vitro mechanical assessment of 2.0-mm system three-dimensional miniplates in anterior mandibular fractures. International Journal of Oral and Maxillofacial Surgery 2014;43(5):564–71.
[152] Qin M, Liu Y, Wang L, He J, Xuan M, Hua C, et al. Design and optimization of the fixing plate for customized mandible implants. J Cranio-Maxillofacial Surg 2015;43(7):1296–302.
[153] Lovald ST, Wagner JD, Baack B. Biomechanical optimization of bone plates used in rigid fixation of mandibular fractures. J Oral Maxillofac Surg 2009;67(5):973–85.
[154] Lovald S, Baack B, Gaball C, Olson G, Hoard A. Biomechanical optimization of bone plates used in rigid fixation of mandibular symphysis fractures. J Oral Maxillofac Surg 2010;68(8):1833–41.
[155] Li C-H, Wu C-H, Lin C-L. Design of a patient-specific mandible reconstruction implant with dental prosthesis for metal 3D printing using integrated weighted topology optimization and finite element analysis. J Mech Behav Biomed Mater 2020:105.
[156] Liu Y-F, Fan Y-Y, Jiang X-F, Baur DA. A customized fixation plate with novel structure designed by topological optimization for mandibular angle fracture based on finite element analysis. Biomed Eng Online 2017;16:131. https://doi.org/10.1186/s12938-017-0422-z.
[157] Şensoy AT, Kaymaz I, Ertas U. Biomechanical evaluation of a novel mandibular distraction osteogenesis protocol: an in-vitro validation and the practical use of the method. Comput Methods Biomech Biomed Eng 2020:1–12.
[158] Wu C, Zheng KK, Fang JG, Steven GP, Li Q. Time-dependent topology optimization of bone plates considering bone remodeling. Comput Methods Appl Mech Eng 2020:359.
[159] Ouyang H, Deng Y, Xie P, Yang Y, Jiang B, Zeng C, et al. Biomechanical comparison of conventional and optimised locking plates for the fixation of intraarticular calcaneal fractures: a finite element analysis. Comput Methods Biomech Biomed Eng 2017;20(12):1339–49.
[160] Al-Tamimi AA, Fernandes PRA, Peach C, Cooper G, Diver C, Bartolo PJ. Metallic bone fixation implants: a novel design approach for reducing the stress shielding phenomenon. Virtual Phys Prototyp 2017;12(2):141–51.
[161] Al-Tamimi AA, Peach C, Fernandes PR, Cseke A, Bartolo PJDS. Topology optimization to reduce the stress shielding effect for orthopedic applications. Procedia CIRP 2017;65:202–6.
[162] Al-Tamimi AA, Huang B, Vyas C, Hernandez M, Peach C, Bartolo P. Topology optimised metallic bone plates produced by electron beam melting: a mechanical and biological study. International Journal of Advanced Manufacturing Technology 2019;104(1–4):195–210.
[163] Al-Tamimi AA, Quental C, Folgado J, Peach C, Bartolo P. Stress analysis in a bone fracture fixed with topology-optimised plates. Biomech Model Mechanobiol 2020;19(2):693–9.
[164] Son D-S, Mehboob H, Chang S-H. Simulation of the bone healing process of fractured long bones applied with a composite bone plate with consideration of the blood vessel growth. Compos B Eng 2014;58:443–50.
[165] Tepic S, Perren SM. The biomechanics of the PC-Fix internal fixator. Injury 1995:26. p. B5-B10.
[166] Sommer C, Gautier E, Müller M, Helfet DL, Wagner M. First clinical results of the locking compression plate (LCP). Injury 2003;34:43–54.
[167] Gautier E, Sommer C. Guidelines for the clinical application of the LCP. Injury 2003;34:63–76.
[168] Bidanda B, Bártolo PJ. Virtual prototyping & bio manufacturing in medical applications. Switzerland: Springer International Publishing; 2021.
[169] Zhang H, Takezawa A, Ding XH, Xu SP, Duan PY, Li H, et al. Bi-material microstructural design of biodegradable composites using topology optimization. Mater Des 2021:209.
[170] Zhang H, Takezawa A, Ding XH, Xu SP, Li H, Guo HH. Topology optimization of degradable composite structures with time-changeable stiffness. International Journal for Numerical Methods in Engineering 2021;122(17):4751–73.
[171] Zhang H, Ding X, Guo H, Xu S, Li H, Nishiwaki S, et al. Multiscale topology optimization of biodegradable metal matrix composite structures for additive manufacturing. Appl Math Model 2023;114:799–822.
[172] Zhang H, Takezawa A, Ding X, Zhang X, Xu S, Li H, et al. Robust topology optimization of biodegradable composite structures under uncertain degradation rates. Compos Struct 2022;291:115593.
[173] Gabarre S, Albareda J, Gracia L, Puértolas S, Ibarz E, Herrera A. Influence of gap size, screw configuration, and nail materials in the stability of anterograde reamed intramedullary nail in femoral transverse fractures. Injury 2017;48:S40–6.
[174] Mehboob A, Mehboob H, Chang S-H, Tarlochan F. Effect of composite intramedullary nails (IM) on healing of long bone fractures by means of reamed and unreamed methods. Compos Struct 2017;167:76–87.
[175] Son D-S, Mehboob H, Jung H-J, Chang S-H. The finite element analysis for endochondral ossification process of a fractured tibia applied with a composite IM-rod based on a mechano-regulation theory using a deviatoric strain. Compos B Eng 2014;56:189–96.
[176] Anderson RT, Pacaccio DJ, Yakacki CM, Carpenter RD. Finite element analysis of a pseudoelastic compression-generating intramedullary ankle arthrodesis nail. J Mech Behav Biomed Mater 2016;62:83–92.
[177] Yakacki CM, Khalil HF, Dixon SA, Gall K, Pacaccio DJ. Compression forces of internal and external ankle fixation devices with simulated bone resorption. Foot Ankle Int 2010;31(1):76–85.
[178] Yakacki CM, Gall K, Dirschl DR, Pacaccio DJ. Pseudoelastic intramedullary nailing for tibio–talo–calcaneal arthrodesis. Expert Review of Medical Devices 2011;8(2):159–66.
[179] Griffin MJ, Coughlin MJ. Evaluation of midterm results of the panta nail: an active compression tibiotalocalcaneal arthrodesis device. J Foot Ankle Surg 2018;57(1):74–80.
[180] Karakaşli A, Satoğlu İ S, Havitçioğlu H. A new intramedullary sustained dynamic compression nail for the treatment of long bone fractures: a biomechanical study. Eklem Hastalik Cerrahisi 2015;26(2):64–71.
[181] Arnone JC, Crist BD, Ward CV, El-Gizawy AS, Pashuck T, Della Rocca GJ. Variability of human femoral geometry and its implications on nail design. Injury 2020.
[182] Cui Y, Xing W, Pan Z, Kong Z, Sun L, Sun L, et al. Characterization of novel intramedullary nailing method for treating femoral shaft fracture through finite element analysis. Exp Ther Med 2020;20(2):748–53.
[183] Plenert T, Garlichs G, Nolte I, Harder L, Hootak M, Kramer S, et al. Biomechanical comparison of a new expandable intramedullary nail and conventional intramedullary nails for femoral osteosynthesis in dogs. PLoS One 2020;5:15.
[184] Putame G, Pascoletti G, Terzini M, Zanetti EM, Audenino AL. Mechanical behavior of elastic self-locking nails for intramedullary fracture fixation: a numerical analysis of innovative nail designs. Front Bioeng Biotechnol 2020:8.
[185] Shibuya N, Manning SN, Meszaros A, Budny AM, Malay DS, Yu GV. A compression force comparison study among three staple fixation systems. J Foot Ankle Surg 2007;46(1):7–15.
[186] Russell SM. Design considerations for Nitinol bone staples. J Mater Eng Perform 2009;18(5):831–5.
[187] Cao L-H, Xu S-G, Wu Y-L, Zhang C-C. Treatment of nonunion of scaphoid waist with Ni-Ti shape-memory alloy connector and iliac bone graft. J Mater Eng Perform 2011;20(4):629–31.
[188] Liu X, Xu S, Zhang C, Su J, Yu B. Application of a shape-memory alloy internal fixator for treatment of acetabular fractures with a follow-up of two to nine years in China. Int Orthop 2010;34(7):1033–40.
[189] Chen X, Liu P, Zhu X, Cao L, Zhang C, Su J. Design and application of Nickel-Titanium olecranon memory connector in treatment of olecranon fractures: a prospective randomized controlled trial. Int Orthop 2013;37(6):1099–105.
[190] Liu X-W, Shang H-J, Xu S-G, Wang Z-W, Zhang C-C, Fu Q-G. Patellar shape-memory Fixator for the Treatment of comminuted Fractures of the inferior Pole of the patella. J Mater Eng Perform 2011;20(4):623–8.
[191] Li H, Mao Y, Qu X, Zhao X, Dai K, Zhu Z. Nickel-titanium shape-memory sawtooth-arm embracing Clamp for complex femoral revision hip arthroplasty. J Arthroplasty 2016;31(4):850–6.
[192] Ko C, Yang M, Byun T, Lee S-W. Design factors of femur fracture fixation plates made of shape memory alloy based on the Taguchi method by finite element analysis. International Journal for Numerical Methods in Biomedical Engineering 2018;5:34.
[193] c J, Su X, w Liu, B -q Yu, Z -d Li, Li M, et al. Shape memory Ni-Ti alloy swan-like bone connector for treatment of humeral shaft nonunion. Int Orthop 2010;34(3):369–75.
[194] Fu QG, Liu XW, Xu SG, Li M, Zhang CC. Stress-shielding Effect of Nitinol swan-like memory compressive Connector on fracture Healing of upper limb. J Mater Eng Perform 2009;18(5):797–804.
[195] w X, Liu S, g Xu, Wang P-f, Zhang C-c. Treatment of clavicular nonunions with shape memory Ni-Ti alloy swan-like bone connector. J Mater Eng Perform 2011;20(4):632–6.
[196] Xu S-G, Zhang C-C, Wu Y-L, Fu Q-G. Swan-like memory compressive connector. J Mater Eng Perform 2011;20(1):139–42.
[197] Mobarak MH, Islam MA, Hossain N, Al Mahmud MZ, Rayhan MT, Nishi NJ, et al. Recent advances of additive manufacturing in implant fabrication – a review. Applied Surface Science Advances 2023;18:100462.
[198] Meng M, Wang J, Huang H, Liu X, Zhang J, Li Z. 3D printing metal implants in orthopedic surgery: methods, applications and future prospects. Journal of Orthopaedic Translation 2023;42:94–112.
[199] Tilton M, Lewis GS, Bok Wee H, Armstrong A, Hast MW, Manogharan G. Additive manufacturing of fracture fixation implants: design, material characterization, biomechanical modeling and experimentation. Addit Manuf 2020;33:101137.
[200] Wang X, Xu S, Zhou S, Xu W, Leary M, Choong P, et al. Topological design and additive manufacturing of porous metals for bone scaffolds and orthopaedic implants: a review. Biomaterials 2016;83:127–41.
[201] Aufa AN, Hassan MZ, Ismail Z. Recent advances in Ti-6Al-4V additively manufactured by selective laser melting for biomedical implants: prospect development. Journal of Alloys and Compounds 2022;896:163072.

[202] Gu DD, Meiners W, Wissenbach K, Poprawe R. Laser additive manufacturing of metallic components: materials, processes and mechanisms. International Materials Reviews 2012;57(3):133–64.
[203] Jawed SF, Rabadia CD, Khan MA, Khan SJ. Effect of alloying elements on the compressive mechanical properties of biomedical titanium alloys: a systematic review. ACS Omega 2022;7(34):29526–42.
[204] Wu G-H, Hsu S-h. *Review: polymeric-based 3D Printing for tissue engineering.* Journal of medical and biological engineering 2015;35(3):285–92.
[205] Mehboob A, Mehboob H, Nawab Y, Hwan Chang S. Three-dimensional printable metamaterial intramedullary nails with tunable strain for the treatment of long bone fractures. Mater Des 2022;221:110942.
[206] Peng B, Xu H, Song F, Wen P, Tian Y, Zheng Y. Additive manufacturing of porous magnesium alloys for biodegradable orthopedic implants: process, design, and modification. J Mater Sci Technol 2024;182:79–110.
[207] Chowdhury S, Arunachalam N. Surface functionalization of additively manufactured titanium alloy for orthopaedic implant applications. J Manuf Process 2023;102:387–405.
[208] Calazans Neto JV, Reis ACd, Valente MLdC. Osseointegration in additive-manufactured titanium implants: a systematic review of animal studies on the need for surface treatment. Heliyon 2023;9(6):17105.
[209] Germaini M-M, Belhabib S, Guessasma S, Deterre R, Corre P, Weiss P. Additive manufacturing of biomaterials for bone tissue engineering – a critical review of the state of the art and new concepts. Prog Mater Sci 2022;130:100963.
[210] Wang R, Ni S, Ma L, Li M. Porous construction and surface modification of titanium-based materials for osteogenesis: a review. Front Bioeng Biotechnol 2022:10.
[211] Chen T, Deng Z, Liu D, Zhu X, Xiong Y. Bioinert TiC ceramic coating prepared by laser cladding: microstructures, wear resistance, and cytocompatibility of the coating. Surf Coating Technol 2021:423.
[212] Chen QX, Jiang YQ, Zhu XL, Zhu TT, Yang LJ, Liu HH, et al. Preparation of HT/PLA coatings on Zn-Mn-Mg alloy surface for biomaterials in bone tissue engineering. Surf Coating Technol 2024:484.
[213] Penkov OV, Pukha VE, Starikova SL, Khadem M, Starikov VV, Maleev MV, et al. Highly wear-resistant and biocompatible carbon nanocomposite coatings for dental implants. Biomaterials 2016;102:130–6.
[214] Leonard JS, Judith AG. Cytotoxic effect of vanadium and oil-fired fly ash on hamster tracheal epithelium. Environ Res 1984;34(2):390–402.
[215] Okazaki Y, Rao S, Tateishi T, Ito Y. Cytocompatibility of various metal and development of new titanium alloys for medical implants. Materials Science and Engineering a-Structural Materials Properties Microstructure and Processing 1998;243(1–2):250–6.
[216] Ramasamy P, Sundharam S. Microhardness and corrosion resistance of plasma sprayed bioceramic bilayer coated Ti-6Al-4V implants. Journal of the Australian Ceramic Society 2021;57(2):605–13.
[217] Al-Saadi S, Banerjee PC, Anisur MR, Raman RKS. Hexagonal boron nitride impregnated silane composite coating for corrosion resistance of magnesium alloys for temporary bioimplant applications. Metals 2017;12:7.
[218] Gross KA, Petzold C, Pluduma-LaFarge L, Kumermanis M, Haugen HJ. Structural and chemical hierarchy in hydroxyapatite coatings. Materials 2020;19:13.
[219] Iqbal N, Iqbal S, Iqbal T, Bakhsheshi-Rad HR, Alsakkaf A, Kamil A, et al. Zinc-doped hydroxyapatite-zeolite/polycaprolactone composites coating on magnesium substrate for enhancing in-vitro corrosion and antibacterial performance. Trans Nonferrous Metals Soc China 2020;30(1):123–33.
[220] Jiang JW, Han G, Zheng XS, Chen G, Zhu PZ. Characterization and biocompatibility study of hydroxyapatite coating on the surface of titanium alloy. Surf Coating Technol 2019;375:645–51.
[221] Shanmugam S, Gopal B. Copper substituted hydroxyapatite and fluorapatite: synthesis, characterization and antimicrobial properties. Ceram Int 2014;40(10):15655–62.
[222] Ni XH, Zhao QM, Pan XY, Zhao G, Zhu XY, Ren LB, et al. Biocompatibility of a magnesium coating on a titanium surface and its effects on BMSCs. Mater Technol 2022;37(14):3129–39.
[223] Ma LM, Wang XL, Zhao NR, Zhu Y, Qiu ZY, Li QT, et al. Integrating 3D Printing and biomimetic Mineralization for personalized enhanced osteogenesis, angiogenesis, and osteointegration. ACS Appl Mater Interfaces 2018;10(49):42146–54.
[224] Jin GD, Cao HL, Qiao YQ, Meng FH, Zhu HQ, Liu XY. Osteogenic activity and antibacterial effect of zinc ion implanted titanium. Colloids and Surfaces B-Biointerfaces 2014;117:158–65.
[225] Patil D, Wasson MK, Aravindan S, Vivekanandan P, Rao PV. Antibacterial and cytocompatibility study of modified Ti6Al4V surfaces through thermal annealing. Materials Science and Engineering C-Materials for Biological Applications 2019;99:1007–20.
[226] Ungureanu C, Dumitriu C, Popescu S, Enculescu M, Tofan V, Popescu M, et al. Enhancing antimicrobial activity of TiO_2/Ti by torularhodin bioinspired surface modification. Bioelectrochemistry 2016;107:14–24.
[227] Lu XX, Wu ZC, Xu KH, Wang XW, Wang S, Qiu H, et al. Multifunctional coatings of titanium implants toward promoting osseointegration and preventing infection: recent developments. Front Bioeng Biotechnol 2021:9.
[228] Konopka K, Goślinski T. Photodynamic therapy in dentistry. J Dent Res 2007;86:694–707.